Gondwana Research 23 (2013) 1378–1401

Contents lists available at SciVerse ScienceDirect

Gondwana Research

journal homepage: www.elsevier.com/locate/gr

Tectonics of the North Qilian orogen, NW China

Shuguang Song [a,*], Yaoling Niu [b,c], Li Su [d], Xiaohong Xia [a]

[a] MOE Key Laboratory of Orogenic Belts and Crustal Evolution, School of Earth and Space Sciences, Peking University, Beijing 100871, China
[b] School of Earth Sciences, Lanzhou University, Lanzhou 730000, China
[c] Department of Earth Sciences, Durham University, Durham DH1 3LE, UK
[d] Geological Lab Center, China University of Geosciences, Beijing 100083, China

ARTICLE INFO

Article history:
Received 12 June 2011
Received in revised form 31 January 2012
Accepted 3 February 2012
Available online 14 February 2012

Keywords:
Oceanic suture zone
Ophiolite
Arc and back-arc basin
High-pressure metamorphism
Subduction and collision
Qilian Orogen

ABSTRACT

The Qilian Orogen at the northern margin of the Tibetan Plateau is a type suture zone that recorded a complete history from continental breakup to ocean basin evolution, and to the ultimate continental collision in the time period from the Neoproterozoic to the Paleozoic. The Qilian Ocean, often interpreted as representing the "Proto-Tethyan Ocean", may actually be an eastern branch of the worldwide "Iapetus Ocean" between the two continents of Baltica and Laurentia, opened at ≥710 Ma as a consequence of breakup of supercontinent Rodinia.

Initiation of the subduction in the Qilian Ocean probably occurred at ~520 Ma with the development of an Andean-type active continental margin represented by infant arc magmatism of ~517–490 Ma. In the beginning of Ordovician (~490 Ma), part of the active margin was split from the continental Alashan block and the Andean-type active margin had thus evolved to western Pacific-type trench–arc–back-arc system represented by the MORB-like crust (i.e., SSZ-type ophiolite belt) formed in a back-arc basin setting in the time period of ~490–445 Ma. During this time, the subducting oceanic lithosphere underwent LT-HP metamorphism along a cold geotherm of ~6–7 °C/km.

The Qilian Ocean was closed at the end of the Ordovician (~445 Ma). Continental blocks started to collide and the northern edge of the Qilian–Qaidam block was underthrust/dragged beneath the Alashan block by the downgoing oceanic lithosphere to depths of ~100–200 km at about 435–420 Ma. Intensive orogenic activities occurred in the late Silurian and early Devonian in response to the exhumation of the subducted crustal materials.

Briefly, the Qilian Orogen is conceptually a type example of the workings of plate tectonics from continental breakup to the development and evolution of an ocean basin, to the initiation of oceanic subduction and formation of arc and back-arc system, and to the final continental collision/subduction and exhumation.

1. Introduction

Plate tectonics through opening and closing of an ocean basin, which is known as the Wilson Cycle (Burke et al., 1976), is the major tectonic scenario on Earth's outer layer and has occurred many times during the Phanerozoic (Condie, 1997). The fragmentation of supercontinent Rodinia in the Neoproterozoic and re-amalgamation into another less long-lived supercontinent Pangaea in the Paleozoic (e.g., Torsvik et al., 1996) manifested such a global cycle. The contemporaneous event occurred widespread in a compound orogenic system in China, i.e., "the Central China Orogenic Belt" (e.g., Jiang et al., 2000), which extends in the W–E direction for approximate 5000 km along the central China mountain chains including Qilian Mountains, Qinling Mountains and Kunlun Mountains.

The Qilian mountain system, which was named "the Sky Mountains" by ancient Hunnish and Chinese people, is located at the northern margin of the Qinghai-Tibetan Plateau, northwestern China. This mountain system, striking in NW–SE direction, is ~100 km wide, ~1000 km long and ~2800 to 5570 m high in altitude. It is offset to the northwest by the Altyn-Tagh Fault, the largest sinistral strike-slip fault in NW China (Fig. 1).

Because of the physiographic difficulty, this mountain system had been poorly studied before the 20th century. From 1920s to 1940s, some Chinese and overseas pioneers set feet in this region for exploration and geological survey on stratigraphy (Yuan, 1925; Bexell, 1935; Hou and Sun, 1935; Sun, 1936; Li, 1946a, 1948a; Guo, 1948), biology (Chi, 1935; Young, 1935; Wang, 1937), igneous petrology (Du Rietz, 1940; Li, 1946b), glacier geology (Weng and Lee, 1946), metamorphism (Sung, 1949; Chen, 1950), tectonics (Lee, 1939; Huang, 1945; Li, 1948a, 1948b; Liang, 1949) and coal and placer gold deposits (Sun, 1940, 1941; He, 1946). Since the establishment of the People's Republic of China in 1949, several geological survey teams have been dispatched to work in the Qilian Mountains for geological

* Corresponding author. Tel.: +86 10 62767729.
E-mail address: sgsong@pku.edu.cn (S. Song).

1342-937X/$ – see front matter © 2012 International Association for Gondwana Research. Published by Elsevier B.V. All rights reserved.
doi:10.1016/j.gr.2012.02.004

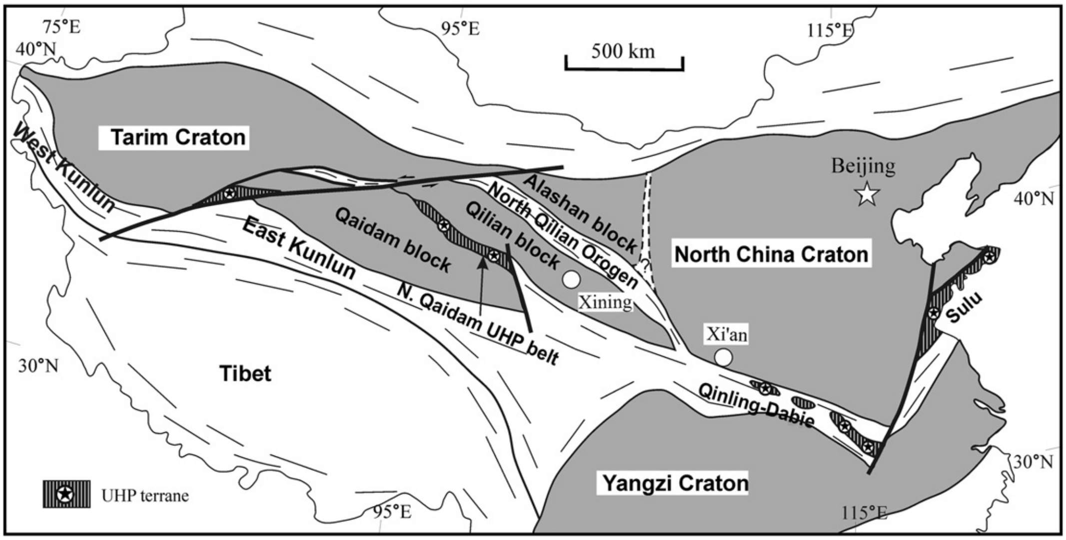

Fig. 1. Schematic maps showing major tectonic units of China.

investigation, mapping and mineral exploration. Several large ore deposits were found and some basic studies on regional geology and mineralization were carried out in this period of time (e.g. Lee, 1954; Lu, 1954; Huang, 1955; Sung, 1955; Yan, 1955; Chen, 1957; Tu, 1957a, 1957b; Hu et al., 1958; Hu, 1959; Institute of Geology of Chinese Academy of Sciences, 1960, 1963).

Since 1970s, the orogenesis of the Qilian Mountains has been reinterpreted in terms of the Plate Tectonics theory as reflected in the studies of ophiolite associations (Wang and Liu 1976, 1981; Xiao et al., 1978; Feng and He, 1995a; Zhang et al., 1997a, 1997b, 1998; Zhang and Zhou, 2001), high-pressure metamorphic rocks (Xiao et al., 1974; Wu, 1980, 1982, 1984, 1987; Zhang and Liou, 1987; Zhang, 1989; Wu et al., 1990, 1993; Song and Wu, 1992; Wu and Song, 1992; Zhang and Xu, 1995; Song, 1996, 1997; Zhang et al., 1997a, 1997b; Cao and Song, 2009; Cao et al., 2011), volcanic rocks (Xia et al., 1991a, 1991b, 1995a, 1995b, 1996, 2003; Wang et al., 2005), and tectonics/orogenic syntheses (Li et al., 1978; Zuo, 1986; Zuo and Liu, 1987; Liou et al., 1989; Feng and Wu, 1992; Xu et al., 1994; Feng and He, 1996; Sobel and Arnaud, 1999; Yue and Liou, 1999; Yin et al., 2007, 2008; Xiao et al., 2009; Gehrels et al., 2011). The well preserved low grade lawsonite-bearing blueschist and eclogite and carpholite-bearing metapelite afford convincing evidence that the North Qilian HP metamorphic belt records cold oceanic lithosphere subduction with a low geothermal gradient (6–7 °C/km) in the Early Paleozoic (Wu et al., 1990, 1993; Song, 1997; Song et al., 2007; Zhang et al., 2007; Zhang et al., 2009). Therefore, this 1000-km-long orogenic belt has been considered as a type example for an ancient oceanic subduction zone that records the forming and shrinking histories of the proto-Tethyan ocean (e.g., Hou et al., 2006; Gehrels et al., 2011) from seafloor spreading and subduction to the ultimate continental collision. This belt was thought to be the final suture zone conjunction of two continents between segments of Rodinia supercontinent and North China Craton (NCC) (Song et al., 2009a).

Furthermore, the Qilian Orogen records of the earliest "cold" oceanic subduction zone on Earth, yet all these remains little known to the international community. The aim of this paper is to provide a comprehensive review of the geological background and spatiotemporal constraints that allow the reconstruction of the evolution history of the Qilian Orogen in terms of the plate tectonics theory, i.e., from oceanic subduction to continental collision in the early Phanerozoic. We document with new data in this paper (1) the two distinguished belts of ophiolite genetically associated with normal ocean-ridge magmatism and back-arc basin magmatism, respectively, (2) island-arc or continental arc magmatic sequences associated with seafloor subduction, (3) high-pressure (HP) low-temperature (LT) metamorphic rocks with age data and P-T-t path, (4) the Silurian flysh and Devonian molasses that indicate ocean basin closing and mountain building processes in response to the continental collision event.

2. Tectonic settings and subunits

The Qilian orogenic belt is part of the Qinling–Qilian–Kunlun Fold System (Li et al., 1978), or the Central China orogenic belt (Fig. 1). It is located in a joint region among the three major blocks in China, i.e., the North China Craton in the northeast, the Yangtze Craton in the southeast and the Tarim Craton in the northwest. The bulldozer-like, northward compression of the Indian Plate led the movement and rotation along the Altyn-Tagh Fault in the Cenozoic, which have re-shaped both topographic and tectonic patterns of the Qilian and adjacent regions.

The Qilian–Qaidam region at the northern Qinghai-Tibet Plateau consists of five nearly E–W trending subparallel tectonic units (Fig. 1); from north to south, they are (1) the Alashan block, (2) the North Qilian orogenic belt (oceanic-type suture zone), (3) the Qilian block, (4) the North Qaidam continental-type UHPM belt, and (5) the Qaidam block. These units were offset by the left-lateral Altyn Tagh Fault system for up to 400 km (Yang et al., 2001; Zhang et al., 2001a, 2001b), although a different view exists (Liu et al., 2009).

2.1. Alashan block

The Alashan block is a triangle-shaped block and has long been considered to be the western part of the North China Craton (e.g. Zhao, 2009). Geographically, it is a desert-covered area with fault-bounded massifs. This block consists predominantly of early Precambrian basement with 2.3–1.9 Ga tonalitic/granitic gneisses (Li et al., 2004a, 2004b; Xiu et al., 2004; Geng et al., 2006) and is overlain by Cambrian to middle Ordovician cover sequences (NBGMR, 1990). The Achean basement is signified by the ~2.7 Ga amphibolite in the northeast part of the block (Geng et al., 2006), as well as by some 2.5–3.5 Ga detrital zircons from meta-sedimentary sequences (e.g. Geng et al., 2007; Tung et al., 2007a, 2007b).

In the northern part of the block, 845–971 Ma foliated granites have been found to intrude the Paleoproterozoic gneisses (Wan et al., 2001; Geng et al., 2002). The famous Jinchuan ultramafic intrusion that contains the world's third largest magmatic Ni–Cu sulfide deposit occurs in the Longshoushan region of the southern part of the Alashan block (e.g. Chai and Naldrett, 1992; Tang et al., 1992). U–Pb zircon analyses yielded ages of 827 ± 8 Ma for the sulfide-bearing ultramafic rocks and 828 ± 3 Ma for the associated dolerite dykes (Li et al., 2004a, 2004b, 2005). This ultramafic intrusion, together with the synchronous mafic dyke swarm, has been suggested to be the product of a superplume that triggered the breakup of the supercontinent Rodinia in the Neoproterozoic around 830–750 Ma (Li et al., 2005).

In summary, Alashan block has a much different tectonic history from the North China Craton, especially in the Neoproterozoic and Early Paleozoic eras. It is therefore unlikely to be the western part of the North China Craton although amalgamation time between these two blocks is unclear at present.

2.2. North Qilian orogenic belt

The North Qilian orogenic belt is an elongate, NW–SE-trending belt that lies between the Alashan Block (north) and the Qilian Block (south) (Fig. 1). This belt is a typical oceanic suture zone and contains Neoproterozoic to Early Paleozoic ophiolite sequences, HP metamorphic belts, island-arc volcanic rocks and granitoid plutons, Silurian flysch formations, Devonian molasse, and Carboniferous to Triassic sedimentary cover sequences. Recent findings of lawsonite-bearing eclogite and carpholite-bearing meta-pelite (Song et al., 2007; Zhang et al., 2007) indicate that the North Qilian orogenic belt records one of the earliest "cold" oceanic lithosphere subduction with a low geothermal gradient (6–7 °C/km) on Earth (see subsequent discussion).

2.3. Qilian block

The Qilian Block, located between the North Qilian orogenic belt and the North Qaidam UHPM belt, is an imbricate thrust belt of Precambrian basement overlain by Paleozoic sedimentary sequences. The basement consists of granitic gneiss, marble, amphibolite and minor granulite. Garnet-bearing (S-type) granite intrusions from the Qilian Block have protolith ages of 880–940 Ma (Guo et al., 1999; Wan et al., 2001; Tung et al., 2007a, 2007b; Xu et al., 2007), similar to ages of the granitic gneisses in the North Qaidam UHPM Belt. Zircons from migmatitic granite give a U–Pb TIMS age of 2469 Ma (Wang and Chen, 1987), and the Paleoproterozoic granitic gneiss of ~2470 ± 20 Ma have been recognized recently in the Qilian Block (Chen et al., 2007, 2009a, 2009b).

2.4. North Qaidam continental-type UHPM belt

The North Qaidam UHPM belt, parallel to the North Qilian oceanic-type suture zone, consists of eclogite- and garnet–peridotite-bearing terranes and extends for ~400 km along the north Qaidam Mountains. The overall characteristics of the rock assemblages, UHP metamorphic evolution and zircon ages suggest that the North Qaidam UHPM belt represents a *continental-type* subduction zone in the Early Paleozoic (see Yang et al., 2002; Song et al., 2003a, 2003b, 2004a, 2005, 2006, 2009c; Mattinson et al., 2006, 2007; Zhang et al., 2006; Yin et al., 2007; Yu et al., 2012). The protoliths of the UHP metamorphic rocks include (1) granitic gneisses with magmatic ages of ~1200–900 Ma (Lu, 2002; Chen et al., 2009a, 2009b); (2) pelitic gneisses with detrital zircon ages of 2400–800 Ma (Song et al., 2006); (3) eclogite blocks with protoliths of 550–500 Ma ophiolite (Zhang et al., 2008) and ~850 Ma continental flood basalts (Song et al., 2010).

Reliable zircon U–Pb ages indicate that the HP-UHP metamorphism and subsequent exhumation occurred from ~460 Ma to 400 Ma (Song et al., 2003a, 2005, 2006; Mattinson et al., 2006, 2009; Zhang et al., 2008; Chen et al., 2009a, 2009b). On the basis of the geochemistry and age data, Song et al. (2006, 2009c) concluded that this UHPM belt is a product of continental deep subduction dragged by the former downgoing oceanic lithosphere (~500–440 Ma) of the Qilian Ocean to depths of 100–200 km at ~430–420 Ma with final exhumation at ~400 Ma. Consequently, this UHPM belt and the North Qilian oceanic suture zone may actually represent tectonic evolution from oceanic subduction to continental collision, to continental underthrusting, and to the final exhumation.

2.5. Qaidam block

The Qaidam Block in the south is a Mesozoic to Cenozoic intracontinental basin with strata deposited on the Precambrian crystalline basement although the thickness of the sediments is poorly known. Some high-grade metamorphic rocks including marble, granulite and felsic gneisses crop out in the southern margin of the block, and are intruded by late Paleozoic granitiod plutons (Wang and Chen, 1987; QBGMR, 1991). Zircon dating (Zhang et al., 2003a, 2003b) revealed that these high-grade rocks have a metamorphic age of ~460 Ma with inherited provenance (detrital) ages of 1800–1600 Ma.

3. Ophiolite sequences in the North Qilian orogenic belt

Ophiolite, a series of rock assemblage formed at seafloor spreading centers of either an open ocean or a back-arc basin (Coleman, 1977), is ubiquitous in the 1000-km-long belt from southeastern end in Jingtai, the North Qilian Mountains, to the northwestern end in Hongliugou, the North Altun. These well-preserved ophiolite sequences have long been considered to represent the oceanic lithosphere of the ancient Qilian ocean (e.g., Xiao et al., 1978; Feng and He, 1995a, 1995b, 1996; Xia et al., 1995a, 1995b, 2003; Zhang et al., 1997a, 1997b, 1998; Qian, et al., 1998, 2001; Smith and Yang, 2006; Tseng et al., 2007). On the basis of Sr, Nd and Pb isotopic data, Hou et al. (2006) suggested that these ophiolites were probably formed in the ancient Tethyan domain or represent part of the Proto-Tethyan Ocean system.

Spatially, as shown in Fig. 2, ophoilite sequences in the North Qilian suture zone distribute in two belts: the southern belt and the northern belt. They occur as nappes with boundaries of thrusting faults. Some ophiolite suites in the two belts have been well-documented.

3.1. The Southern Ophiolite Belt—ophiolite of Ocean ridge origin?

The Southern Ophiolite Belt (SOB) extends from Aoyougou in the northwest, via Yushigou, Dongcaohe, to Yongdeng in the southeast (Fig. 2). Petrographic and geochemical studies indicate that basaltic rocks in the southern belt resemble present-day N-type and E-type MORB and therefore have been suggested to represent the oceanic crust generated at an ocean ridge (Feng and He, 1995a, 1995b; Hou et al., 2006; Tseng et al., 2007). Magmatic zircons from cumulated gabbros give U–Pb SHRIMP ages ranging from 496 to 550 Ma (Yang et al., 2002; Shi et al., 2004; Tseng et al., 2007; this study). Three representative ophiolite suites in Aoyougou, Yushigou and Dongcaohe regions have been well documented (see following discussion).

3.1.1. Aoyougou ophiolite suite

The Aoyougou ophiolite suite is located in the western part of the SOB (see Fig. 2 for locality). It consists of dismembered serpentinite, gabbro, and massive and pillow-like basalts (Fig. 3). Xiao et al. (1978) first reported this ophiolite and suggested it to be formed in the Precambrian based on the occurrence that is tectonically intercalated with some Precambrian dolostone sedimentary layers. The forming age, however, is debatable so far. Zhang et al. (2001a, 2001b) reported zircon SHRIMP ages of 1.47–1.78 Ga from amphibolite blocks within the serpentinite, and thus suggested a Proterozoic ophiolite. Xiang et al. (2007) reported much younger zircon SHRIMP ages of 504 ± 6 Ma from a gabbroic sample and thus concluded that

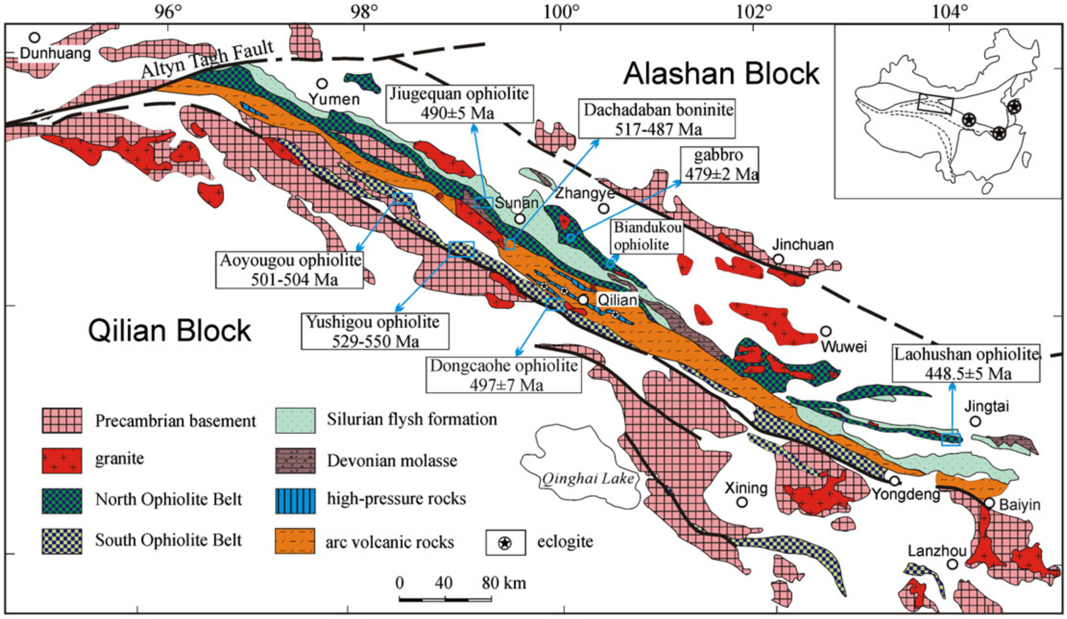

Fig. 2. Geological map of the North Qilian Orogen with localities of major ophiolite suites and their ages.

this ophiolite was formed in the Early Paleozoic rather than in the Proterozoic.

3.1.1.1. Ultramafic rocks. The ultramafic rocks are located in the south of the cross-section. They are completely serpentinized and strongly deformed along the thrusting fault (Fig. 3).

3.1.1.2. Gabbro and dolerite. These rocks occur as a ~400-m thick "layer" in the cross-section (Fig. 3) and are bounded by strongly deformed serpentine schist to the south. From south to north, these rocks vary petrographically from coarse-grained cumulate grabbro to fine-grained homogeneous gabbro and then to dolerite with an ophitic texture. No ultramafic cumulate has been found in this section.

Geochemical analyses show that the fine-grained gabbro and dolerite have a uniform composition with SiO_2<50 wt.%, TiO_2 0.79–1.13, Al_2O_3 14.15–14.37, MgO 6.66–7.72, Na_2O 2.1–2.53 and $Mg^{\#}$ [$=Mg/(Mg+Fe^{2+})$] 0.58–0.65. They have relatively low concentrations of REE and HFSE, and the chondrite-normalized REE patterns are rather flat ($La_N/Yb_N=1.05$–1.24) without a Eu anomaly (Eu^* 0.93–0.96). However, they are enriched in Ba and Sr (Fig. 4a,b).

Mafic lavas (including massive and pillow basalts) are the major component in the upper part of the ophiolite sequence and occur interbedded with layers of Precambrian carbonate. They are subalkaline basalts with high TiO_2 (2.14–3.19 wt.%), Fe_2O_3t (13–17 wt.%) and relatively low $Mg^{\#}$ (0.36–0.45). Their chondrite-normalized REE patterns display LREE enrichment ($La_N/Yb_N=2.96$–4.55) and a weak Eu negative anomaly ($Eu^*=0.80$–0.93). The primitive mantle (PM) normalized multi-element diagram displays similar patterns to present-day E-MROB and OIB (e.g., Sun and McDonough, 1989). All basaltic rocks plot in N-MORB or WPB fields in the traditional discriminant diagrams (Fig. 5). The weak negative anomaly of Nb and Ta relative to Th–U and LREE may be interpreted as a result of continental crustal contamination, similar to typical continental flood basalts. Therefore, field occurrence and geochemistry suggests these basalts are most probably Precambrian CFB, not the member of the Aoyougou ophiolite sequence.

Zircons from one fine-grained gabbro are colorless and show rectangle or irregular shapes with long axes varying from 50 μm to 100 μm and length/width ratios from 1.2 to 1.5. Cathodoluminescent (CL) images display straight and wide oscillatory growth bands, which are interpreted as typical features for zircons from mafic volcanic or gabbroic rocks. The uranium content in zircons from sample Q5–56 varies in a relatively narrow range (239 to 568 ppm); Th varies from 167 to 666 ppm with Th/U ratios of 0.58–1.68. Analyses of 11 zircon grains by SHRIMP yield $^{206}Pb/^{238}U$ apparent ages ranging from 493 to 515 Ma with a weighted mean of 501.4 ± 4.3 Ma (MSWD = 1.09) (Xia et al., in press). This age is consistent with the previous results by Xiang et al. (2007) and thus should represent the forming time of the Aoyougou ophiolite in the Late Cambrian.

3.1.2. Yushigou ophiolite suite

The Yushigou Ophiolite suite (see Fig. 2 for its locality) occurs as a nappe over-thrusting onto the Precambrian crystalline basement of

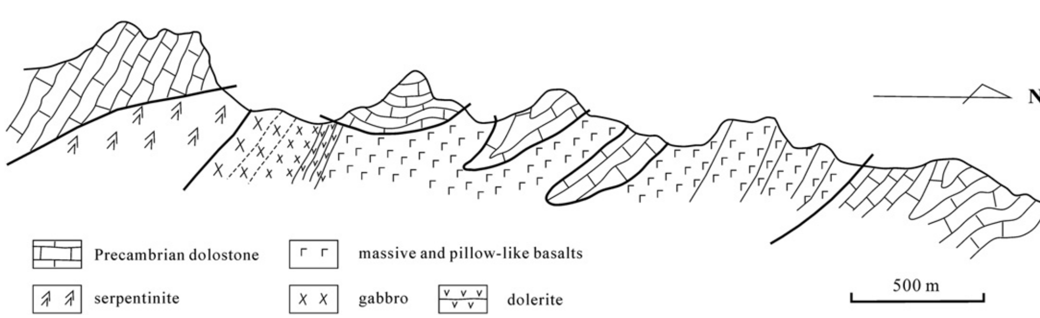

Fig. 3. The cross-section of the Aoyougou ophiolite suite in the west part of the North Qilian Mounatins (modified after Xiang et al., 2007).

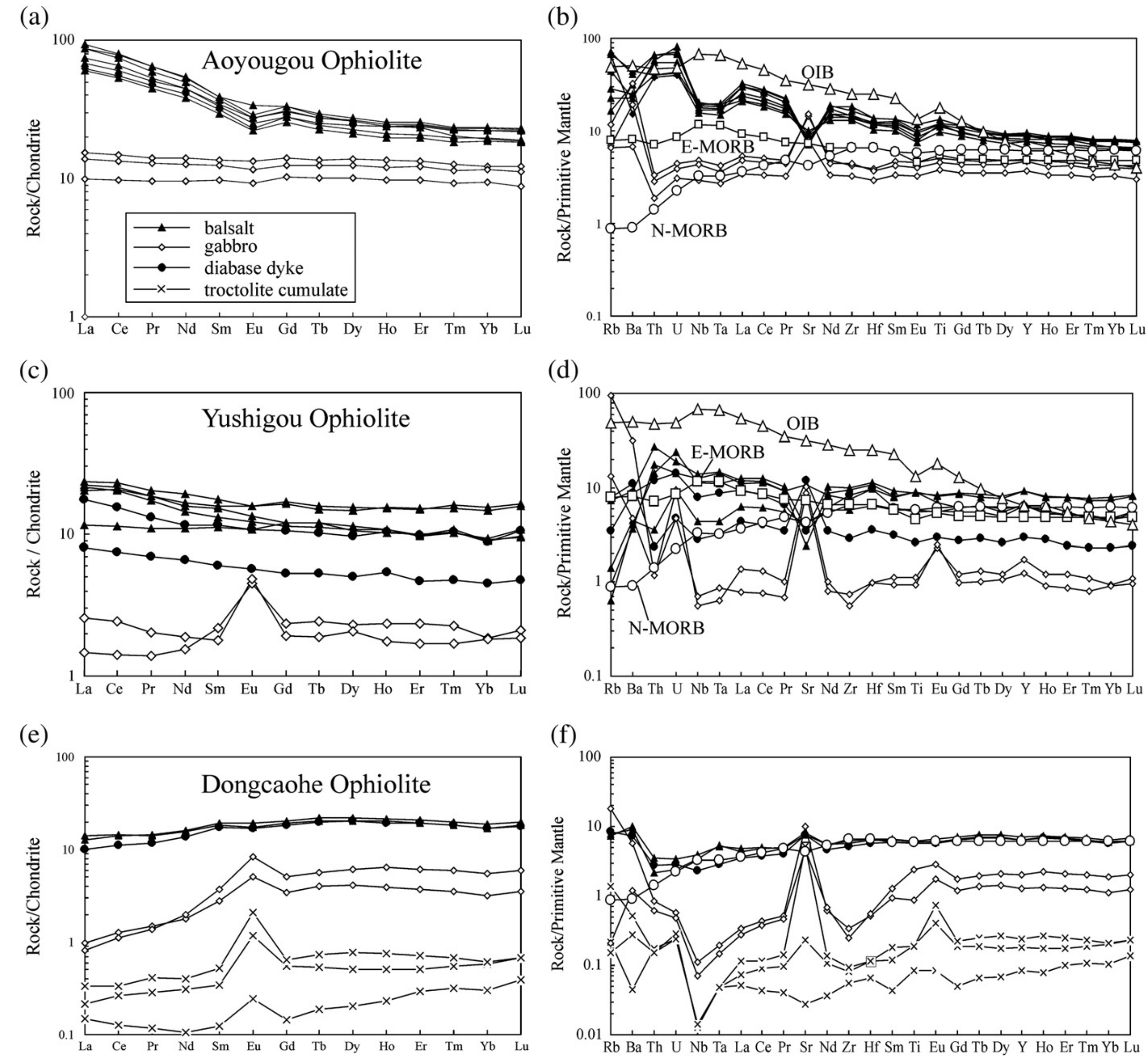

Fig. 4. Chondrite-normalized REE patterns and primitive mantle normalized spidergrams for ophiolite suites from the South Ophiolite Belt. Data of Aoyougou and Yushigou ophiolites (a)–(d) are from this study. Data of Dongcaohe ohpiolite in (e) and (f) are from Tseng et al. (2007).

the Central-Qilian block. It was first described as an ophiolite suite formed in the Cambrian on the basis of fossils in sedimentary rocks of the same sequence by Xiao et al. (1978), and followed by other studies (e.g. Feng and He, 1995a, 1995b; Song and Su, 1998; Shi et al., 2004; Hou et al., 2006; Song et al., 2009b). The rock assemblage in the Yushigou ophiolite consists of mantle peridotite, ultramafic to mafic (gabbroic) cumulate, pillow basalts and sedimentary rocks including marl and reddish radiolarian chert; they compose a complete section of oceanic lithosphere (Fig. 7). Shi et al. (2004) reported a SHRIMP age of 550 ± 17 Ma of zircons from a gabbro.

3.1.2.1. Mantle peridotite. The mantle peridotite is a ~25 km^2 fault-bounded block, the largest mantle slab in the North Qilian suture zone. Since it occurs spatially in the lower part of the Yushigou ophiolite suite, this mantle peridotite was previously interpreted as an element of a highly dismembered Yushigou ophiolite (Song and Su, 1998; Su et al., 1999; Zhang et al., 2003a, 2003b). Harzburgite is the major rock type with minor dunite and pyroxenite occurring as dikes/veins within the harzburgite.

The harzburgite block shows massive coarse-grained inequigranular textures, and comprises olivine (~70–85 vol.%), orthopyroxene (Opx, ~10–25 vol.%), minor clinopyroxene (Cpx, <2–3 vol.%) and Cr-rich spinel (Spl, ≤1.0 vol.%). Compared with abyssal peridotites (AP) from mid-ocean ridges (Dick, 1989; Niu and Hékinian, 1997a, 1997b), the Yushigou harzburgite is much more depleted than the most depleted AP samples, e.g., high Fo (i.e., Mg$^{\#}$, Mg/[Mg + Fe^{2+}] × 100 = 91–93) in olivine and high Cr$^{\#}$ (Cr/[Cr + Al] = 0.58–0.67) in spinel, and resembling highly depleted forearc harzburgites (Song et al., 2009b).

3.1.2.2. Cumulate sequence. Gabbro is the major rock type in the cumulate sequence and shows clear cumulate layers defined by modal variations of plagioclase and clinopyroxene. Two layers of serpentinized dunite, in which a large massive chromitite deposit has been exploited, occur in the bottom of the cumulate sequence. Websterite

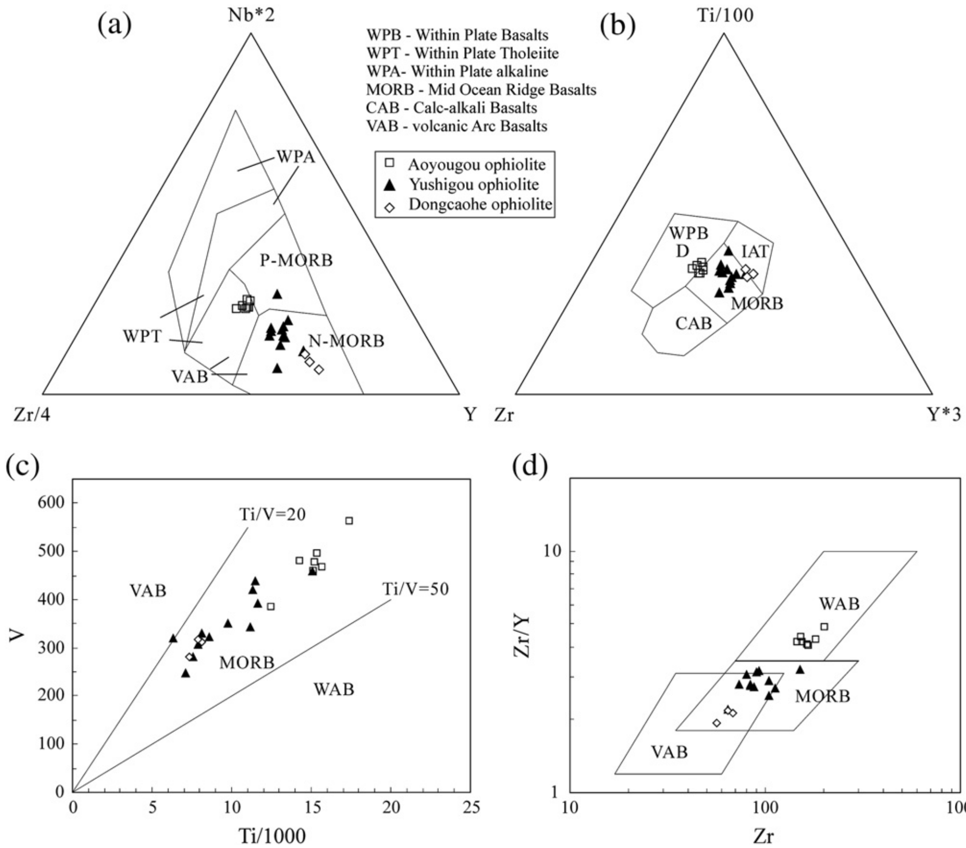

Fig. 5. Discriminant diagrams for basaltic rocks from the Southern Ophiolite Belt. Data of Aoyougou and Yushigou ophiolites are from this study and data of Dongcaohe ophiolite are from Tseng et al. (2007).

and norite layers also occur in the lower part of the sequence. Geochemical analyses show that gabbros are enriched in Ba, Sr and Eu but have relatively low concentrations of REEs and HFSEs as a result of accumulation with higher plagioclase/pyroxene ratios.

Two gabbro samples were chosen for zircon U–Pb geochronological study. Zircon crystals are colorless and euhedral with long axes varying from 100 μm to 200 μm and length/width ratios from 1 to 2. CL images show all zircon crystals from the two samples display straight and wide oscillatory growth bands, which is interpreted as typical features of zircons from gabbroic rocks. The U content in zircons from sample Q5–56 varies in a narrow range from 1290 to 2294 ppm and Th from 759 to 1641 ppm with Th/U ratios of 0.58–0.84. Analyses of 10 zircon grains by SHRIMP yield $^{206}Pb/^{238}U$ apparent ages ranging from 530 to 566 Ma with a weighted mean of 548 ± 9 Ma (MSWD = 1.9). The U content in zircons from sample Q5 to 57, on the other hand, varies significantly from 241 to 3880 ppm and Th from 195 to 5660 ppm with Th/U ratios of 0.76–2.09. The $^{206}Pb/^{238}U$ apparent ages of the 11 zircon grains range from 516 to 555 Ma and yield a weighted mean of 529 ± 9 Ma (Shuguang Song, unpublished data).

3.1.2.3. Pillow basalts. Pillow basalts occur in the southern part of the section and represent the upper section of the ophiolite. The maximum thickness exceeds 4 km in cross-section. Most samples show well-preserved pillows of varying size (~0.2 to 1.5 m in diameters). Some doleritic dikes intrude the pillow basalts.

The pillow basalts are tholeiitic with SiO_2 47.3–51.8 wt.%, TiO_2 1.06–2.52 wt.%, MgO 4.62–8.24 wt.% and $Mg^{\#}$ 0.40–0.64. They display flat and slightly enriched REE patterns (La_N/Yb_N = 1.01–2.56) and a week negative Eu anomaly (Eu/Eu* = 0.77–1.0) (Fig. 4c). In the primitive mantle (PM) normalized multi-element diagram, all pillow basalts show similar patterns to present-day E-MROB (Fig. 4d). One dolerite sample has relatively high MgO (10.15 wt.%), low TiO_2 and total REEs, and Sr enrichment.

3.1.3. Dongcaohe ophiolite

The Dongchaohe ophiolite is located in the middle part of the southern ophiolite belt, ~2 km south of the town of Qilian (see Fig. 2). As documented in details by Tseng et al. (2007), this ophiolite massif can be divided into three sections: (1) the basal cumulate section, (2) the middle isotropic section and (3) the top dyke and lava section. The basal section consists of cyclic layers of cumulate dunites, troctolites, anorthosites, anorthositic gabbros and gabbros with small discordant dunite and troctolite bodies. This layered sequence grades upward to isotropic gabbros and gabbronorites, which are overlain by the extrusive sequence of sheeted dikes and basaltic lavas. These cumulate lithologies suggest the Dongcaohe ophiolite formed in a mid-ocean ridge (MOR) setting.

The whole-rock geochemistry (data are documented from Tseng et al., 2007) shows that the troctolite, anorthosite and gabbro display compositional characteristics of cumulate with low concentrations of REEs and HFSEs and a positive anomaly for Sr and Eu (Fig. 4e,f). The basaltic samples including sheeted dykes and pillow lavas in the top section display typical N-type MORB affinity in both discriminant diagrams (Fig. 5) and normalized REE and multi-element diagrams (Fig. 4e,f). Zircons from the gabbronorite gave a weighted mean $^{206}Pb/^{238}U$ age of 497 ± 7 Ma (Tseng et al., 2007).

3.2. The Northern Ophiolite Belt—ophiolite from the back-arc basin

The Northern Ophiolite Belt (NOB) is located north of the arc-magmatic complex and extends in parallel with the southern belt. Petrographic and geochemical studies show that basaltic rocks in the northern belt geochemically resemble present-day N-type MORB

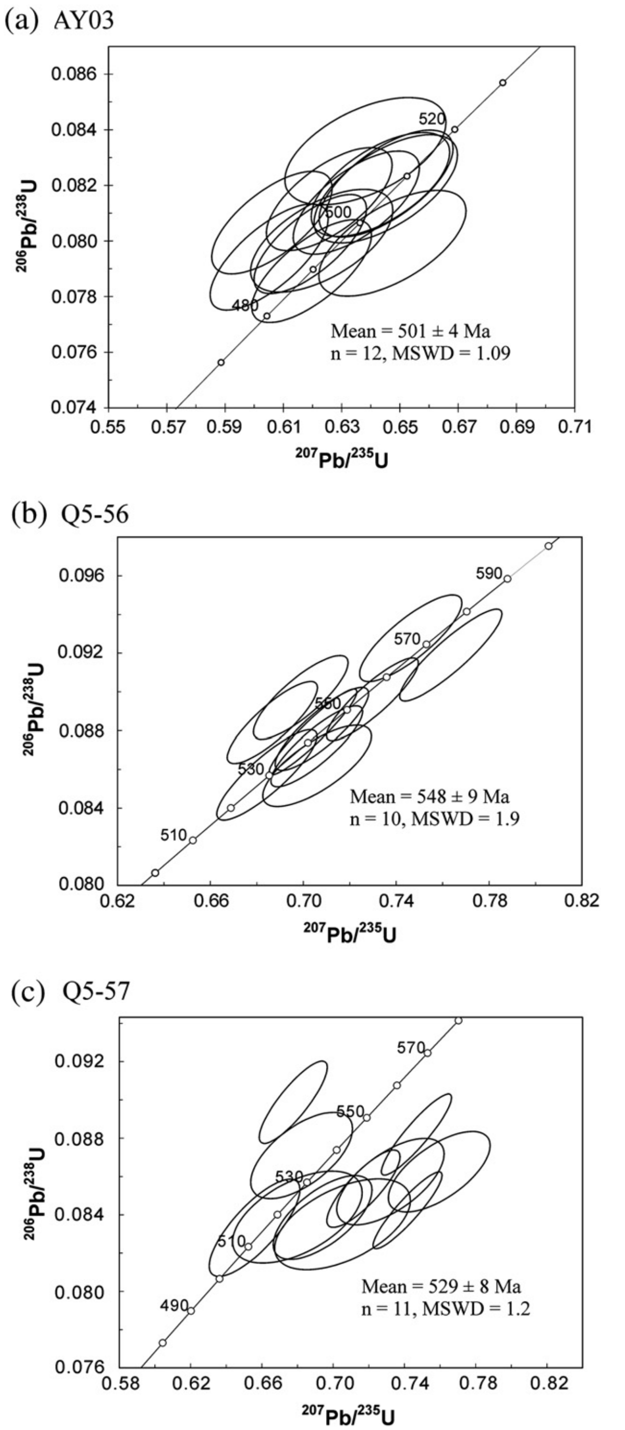

Fig. 6. Concordia diagrams for zircon SHRIMP analyses from gabbroic samples in the South Ophiolite Belt. (a) Sample from the Aoyougou ophiolite suite. (b) and (c) Samples from Yushigou ophiolite suite.

(Qian et al., 2001; Song et al., 2009a), but the rock assemblage suggests that these ophiolite suites are most consistent with formation in a back-arc spreading center (supra-subduction zone (SSZ) type ophiolite) (Qian et al., 2001; Xia et al., 2003; Xia and Song, 2010). Zircons from gabbros in the Northern Ophiolite Belt (NOB) give U–Pb SHRIMP ages ranging from 448 to 490 Ma (Xia and Song, 2010; this study), much younger than ages of the SOB. Three representative ophiolite suites, i.e., the Jiugequan ophiolite in the west, the Biandukou ophiolite in the middle and the Laohushan ophiolite in the far southeast (see Fig. 2 for their localities), are described subsequently.

3.2.1. Jiugequan ophiolite

The Jiugequan ophiolite is located ~40 km southwest of the town of Sunan and extends along the Bailong River (Fig. 8). To its south is the lawsonite-bearing blueschist belt, and to the further south, they thrust southwestwards onto the Devonian molasses. New $^{40}Ar/^{39}Ar$ dating revealed that the blueschist facies metamorphism occurred at 413–415 Ma (Lin et al., 2010). As shown in Fig. 8, the Jiugequan ophiolite consists of gabbro, pillow basalt, dolerite dykes, mafic breccias and minor serpentinized peridotite (mantle peridotite?). The upper part of the ophiolite comprises thick and massive basalt and balsaltic andesite interbedded with pelitic chert and greywacke layers. A Cyprus-type sulfide copper deposit has been mined in this ophiolite suite for many years.

The analyzed eight dolerite dyke and pillow lava samples from Jiugequan Ophiolite span a wide range from basaltic to andesitic (Fig. 9a) with SiO_2 45–57 wt.%, TiO_2 0.44–2.29 wt.% Fe_2O_3 7.7–15 wt.%, MgO 4.5–8.3 wt.% and relatively high and varying $Mg^{\#}$ value (Mg/(Mg + Fe) = 0.46–0.69. They show both tholeiitic and cala-alkaline features in the Alkali–FeOt–MgO (AFM) diagram (Fig. 9b).

Three dolerite samples have lower concentrations of REEs and HFSEs than pillow lavas and show LREE depleted patterns. In the primitive mantle-normalized trace element spidergram (Fig. 10a), all samples show various enrichments in Rb, Ba, Th and U relative to HFSEs. Nearly all samples show a pronounced negative Nb-Ta anomaly and a weak negative Zr–Hf anomaly.

In Zr–Nb–Y discrimination diagram (Fig. 11a), all dolerite-basalt samples are plotted across the N-MORB and VAB fields, and the same result is obtained in other discrimination diagram (Fig.11b–d). All these data suggest that the Jiugequan ophiolite may have formed in a supra-subduction zone (SSZ) environment. In addition, the presence of a high proportion of volcanic breccia and terrigenous-volcanic sedimentary rocks in the Jiugequan ophiolite suggest that this ophiolite most likely formed in a back-arc basin setting related to subduction zone and volcanic arc, rather than the mature ocean spreading setting.

Zircon grains separated from a gabbro sample (08QS60) are fragmented, euhedral crystals with clear and simple concentric oscillatory zoning in CL images. The measured U concentration in zircons is relatively low, ranging from 21 to 204 ppm with varying Th/U ratios of 0.17–3.64. All analyses on 18 grains give concordant $^{206}Pb/^{238}U$ ages of 472 Ma to 508 Ma with a weighted mean of 490 ± 5 Ma (MSWD = 1.06, Fig. 12a), which is interpreted as the crystallization age of the gabbroic cumulate in the Jiugequan ophiolite (Xia and Song, 2010).

3.2.2. Biandukou ophiolite

The Biandukou ophiolite suite is located in the middle part of the North Qilian orogenic belt (see Fig. 2 for locality). It mainly consists of pillow and massive lavas, dyke-like gabbro, and tuff. These volcanic rocks are inter-bedded with a fine-grained sedimentary sequence with siltstone, slate and muddy chert.

The analyzed massive and pillow lavas display a wide compositional range from basaltic to andesitic with SiO_2 44.89–57.45 wt.%, TiO_2 0.36–1.99 wt.% Fe_2O_3t 8.4–12.95 wt.%, MgO 5.61–10.05 wt.% and high $Mg^{\#}$ 0.57–0.76. Most samples show LREE enrichment relative to HREEs (La_N/Yb_N = 2.88–26.44) except for one gabbro and two basalt samples. In the primitive mantle-normalized multi-element spidergram (Fig. 10b), all samples display enrichments in Rb, Ba, Th, U and LREEs relative to HFSEs. Nearly all samples show a pronounced negative Nb-Ta anomaly and a weak negative Zr–Hf anomaly, which resemble features of typical volcanic arc basalts.

Zircons from a gabbro sample (09QL54) in northwest of the Biandukou ophiolite are euhedral with clear and simple concentric oscillatory zoning in CL images. Some zircons contain various inherited cores that have been captured from the basement rocks. Using LA-ICP-MS U–Pb dating method, two cores yield a concordant age of

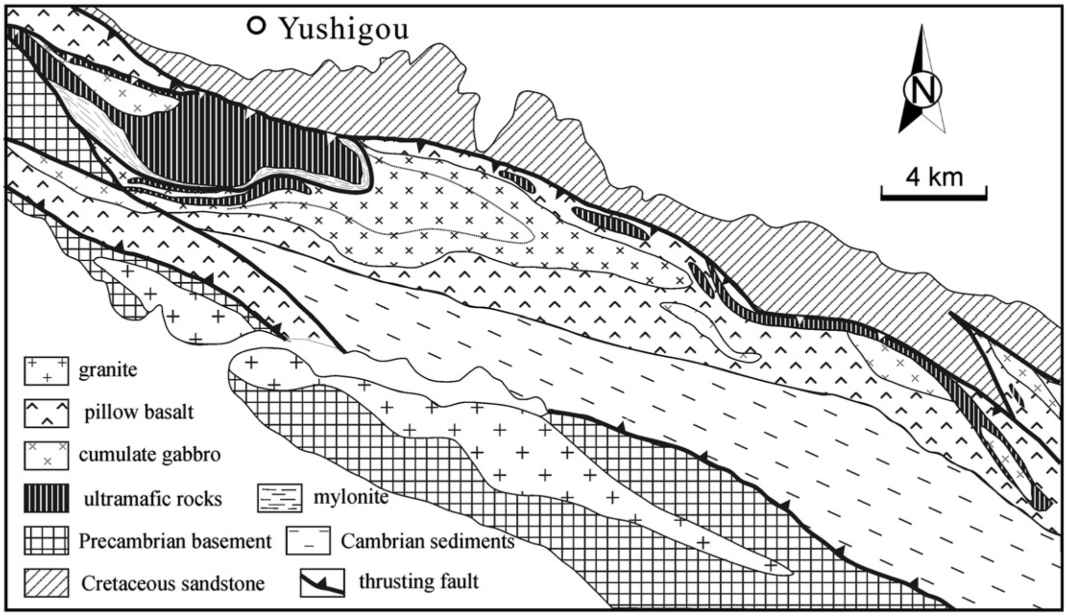

Fig. 7. Geological map of the Yushigou ophiolite suite.

2554 ± 59 Ma, two cores yields Grenvillian ages of 917 Ma and 1256 Ma. These Proterozoic and Archean ages suggest that both the proto arc basement and the back-arc basin were developed from a continental margin (see Niu et al., 2003; Xia et al., in press). Twenty-five zircon grains give $^{206}Pb/^{238}U$ ages of 470–488 Ma with a weighted mean of 479 ± 2 Ma (MSWD = 0.87) (Fig. 12b), which should represent forming age of the ophiolite suite in this region.

3.2.3. Laohushan ophiolite

The Laohushan ophiolite suite is located in the east part of the North Qilian suture zone, ~20 km southwest of the town of Jingtai, Gansu Province (Fig. 2). This ophiolite has been well studied with respect to rock assemblage, geochemistry and forming time by radiolaria and Sm-Nd whole-rock ages (Feng and He, 1996; Xia et al., 1996, 1998, 2003; Zhang et al., 1997a, 1997b; Qian et al., 2001).

As shown in Fig. 13, the rock assemblage of this ophiolite suite consists of serpentinized peridotite, gabbro of ~1.5 km thickness, massive dolerite, pillow lavas and sedimentary rocks. Sedimentary rocks in the upper part of the ophiolite are layers of reddish, radiolarian-bearing muddy chert and slate in varying thickness (from <1 m to up to several 10s of meters); they occur conformably inter-bedded with pillow lavas. To the upper part of the ophiolite, turbidite with rhythm layers of fine-grained sandstone, siltstone and slate increases, suggesting a relatively shallow-water environment. Silurian rudaceous turbidite sequence with conglomerate, sandstone and siltstone is overlain on the top of the ophiolite.

Chemical analyses show that pillow lavas and massive dolerite in the Laohushan ophiolite are mostly sub-alkaline tholeiite with SiO_2 46.61–53.30 wt.%, TiO_2 0.93–4.18 wt.%, and MgO 4.09–11.64 wt.% and variable and high $Mg^{\#}$ value from 0.45 to 0.76. Most basalt samples show weak LREE-enriched patterns with La_N/Yb_N (Chondrite-

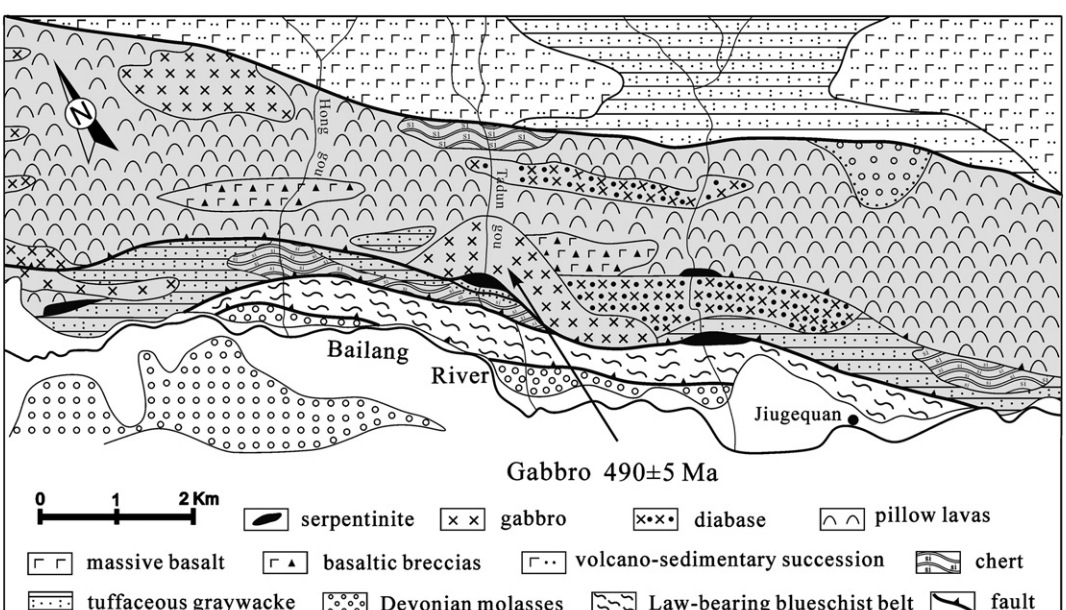

Fig. 8. Geological map of Jiugequan region showing rock assemblage of the SSZ type ophiolite and low-grade blueschist (after Xia and Song, 2010).

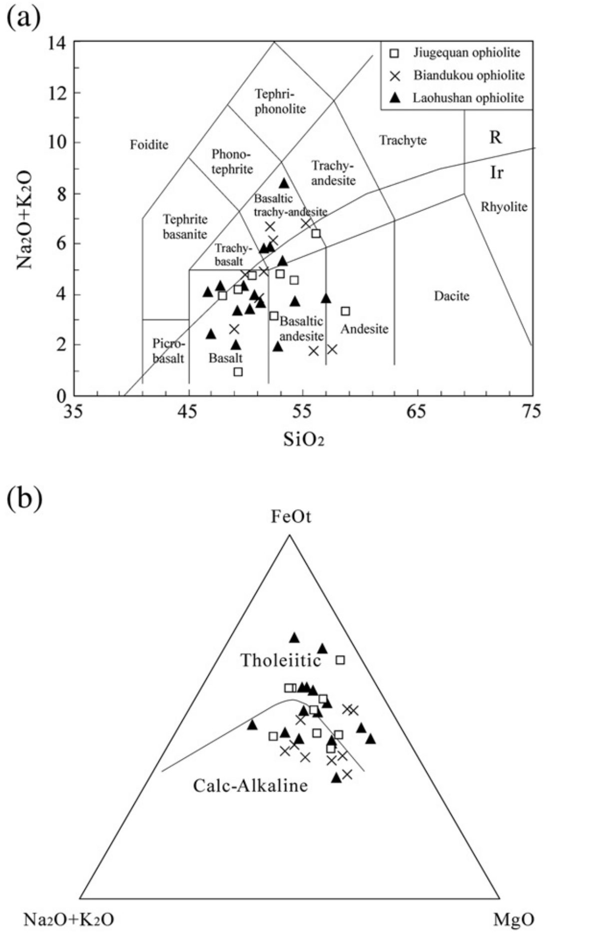

Fig. 9. TAS (a) and AFM (b) diagrams for basaltic rocks from the North Ophiolite Belt.

normalized) 1.07–3.98. In the primitive mantle normalized multi-element diagram, they display similar patterns that resemble present-day N-type and E-type MORBs (Fig. 10c). The coarse-grained gabbro has relatively lower concentrations of REEs than the pillow basalts and a clear positive Eu anomaly, suggesting plagioclase accumulation.

In traditional discrimination diagrams (Fig. 11), such as Nb–Zr–Y (Meschede, 1986), Ti vs. V (Shervais, 1982) and Zr vs. Zr/Y (Pearce and Norry, 1979), most basalt and dolerite samples plot across the MORB, VAB and WPB fields. In the Hf–Th–Ta diagram, samples plot across N-type MORB and VAB fields, suggesting that subduction-zone fluid may have interacted with the basaltic rocks. REE patterns of chert from the Jiugequan ophiolite indicate that they may have formed neither in the vicinity of continental margin nor in a typical open ocean basin, but a back-arc basin (Qian et al., 2001).

Zircon separates from a fine-grained gabbro are colorless and long euhedral crystals with length/width ratios from 2.0 to 6.5. Their CL images display straight and wide oscillatory growth bands, which, together with the euhedral crystal shape, are interpreted as features for zircons from a mafic intrusion. Eleven analyses of 11 zircons were obtained for sample 09LH18. Uranium content varies from 250 to 939 ppm with Th/U ratios of 0.66–1.15. The apparent $^{206}Pb/^{238}U$ ages of the 11 zircon grains range from 438 ± 5 Ma to 456 ± 5 Maand yield a weighted mean of 448.5 ± 4.7 Ma (MSWD = 1.4) (Fig. 12c), similar to Sm–d age of 453.6 ± 4.4 Ma (Xia et al., 2003).

4. Island-arc igneous complex

As shown in Fig. 2, the island-arc igneous complex extends as a continuous belt in between the two ophiolite belts along the major tectonic line of the North Qilian orogenic belt. This igneous complex consists predominantly of (1) boninitic complex, (2) mafic to felsic volcanic complex with Cu–Pb–Zn ore deposits, and (3) various granite/granodiotrite plutons.

4.1. Boninite complex

The boninite complex is located in the Dacha-Daba (DCDB, Daba means mountain ridge) region, ~50 km south of the town of Sunan, the middle part of the North Qilian suture zone (see Fig. 2 for locality). This complex was first described as high-Mg andesite by Xia et al. (1991a, 1991b), later as component of normal oceanic ophiolite by Feng and He (1995a, 1995b), more recently as boninite or boninite-like complex by Chen et al. (1995), Song (1996) and Zhang et al. (1997a, 1997b, 1998). The more recent and comprehensive work by Xia et al. (in press) indicated that this boninite sequence is earliest products of infant arc splitting and subsequent back-arc basin development. Fig. 14 shows the field occurrence and rock assemblage of the boninite complex.

4.1.1. Petrography of the boninite complex

4.1.1.1. Gabbro. Gabbro occurs as several layers inter-bedded with massive dolerite and pillow lavas. They show medium- to fine-grained gabbroic texture. The gabbro has ~65–70 vol.% plagioclase and 25–30 vol.% pyroxene. Most pyroxenes are overprinted by amphibole.

4.1.1.2. Massive dolerite. The massive dolerite is located in the northern part of the cross-section and constitute the lower part of boninite sequence together with the gabbro. Feng and He (1995a, 1995b) interpreted the dolerite as sheeted dykes with single-chilled margins. However, these margins are mostly parallel fractures and the chilling margins are mostly absent. Rather, columnar joints were observed. The rocks show a fine-grained gabbroic or doleritic texture with strong alteration.

4.1.1.3. Pillow lavas. The pillow lavas are the major component of the boninite sequence and crop out about 2200 m in the total thickness in the northern part of cross-section (Fig. 15a,b). Amygdules, usually filled with chlorite, calcite and/or prehnite, crowded together at the outer crusts of the pillows, which are overturned (Fig. 15b). Two layers of gabbro and many single or sheeted dykes intruded the pillow lavas (Fig. 15c,d). In thrusting fault belt, the pillows are strongly flattened and mylonitized. The rocks are characterized by vitrointersitial and spilitic structures and consist of about 35–40% skeletal plagioclase, 15–20% altered pyroxene and 35–40% matrix.

4.1.1.4. Dolerite dykes. Most of the dolerite dykes have single chilled margins and cut the layer of pillow lavas at a high angle. Some are united together as sheeted dyke swarm (Fig. 15c,d).

4.1.1.5. Volcanic tuff. The volcanic tuff, located north of the pillow lavas, is ~500 m in thickness, and consists of about 35% crystal and lithic clasts and 65% tuff matrix.

4.1.2. Geochemistry and forming ages

On the basis of petrography and geochemistry, two groups have been recognized, i.e., the lower tholeiite group and the upper boninite group. The lower tholeiite group, including gabbro and dolerite in the south part of the cross-section, are tholeiitic and similar to the N-type MORB with normal contents of SiO_2 (49–52 wt.%), TiO_2 (>1 wt.%) and MgO (<7.8 wt.%). The upper group, including pillow lavas and doleritic dykes, have high SiO_2 (most in the range of 53–60 wt.%), MgO (7–20 wt.%) but low K_2O (0.1–0.78 wt.%) and very low TiO_2 (0.27–0.44%), showing features of boninite affinity. In SiO_2–($Na_2O + K_2O$)

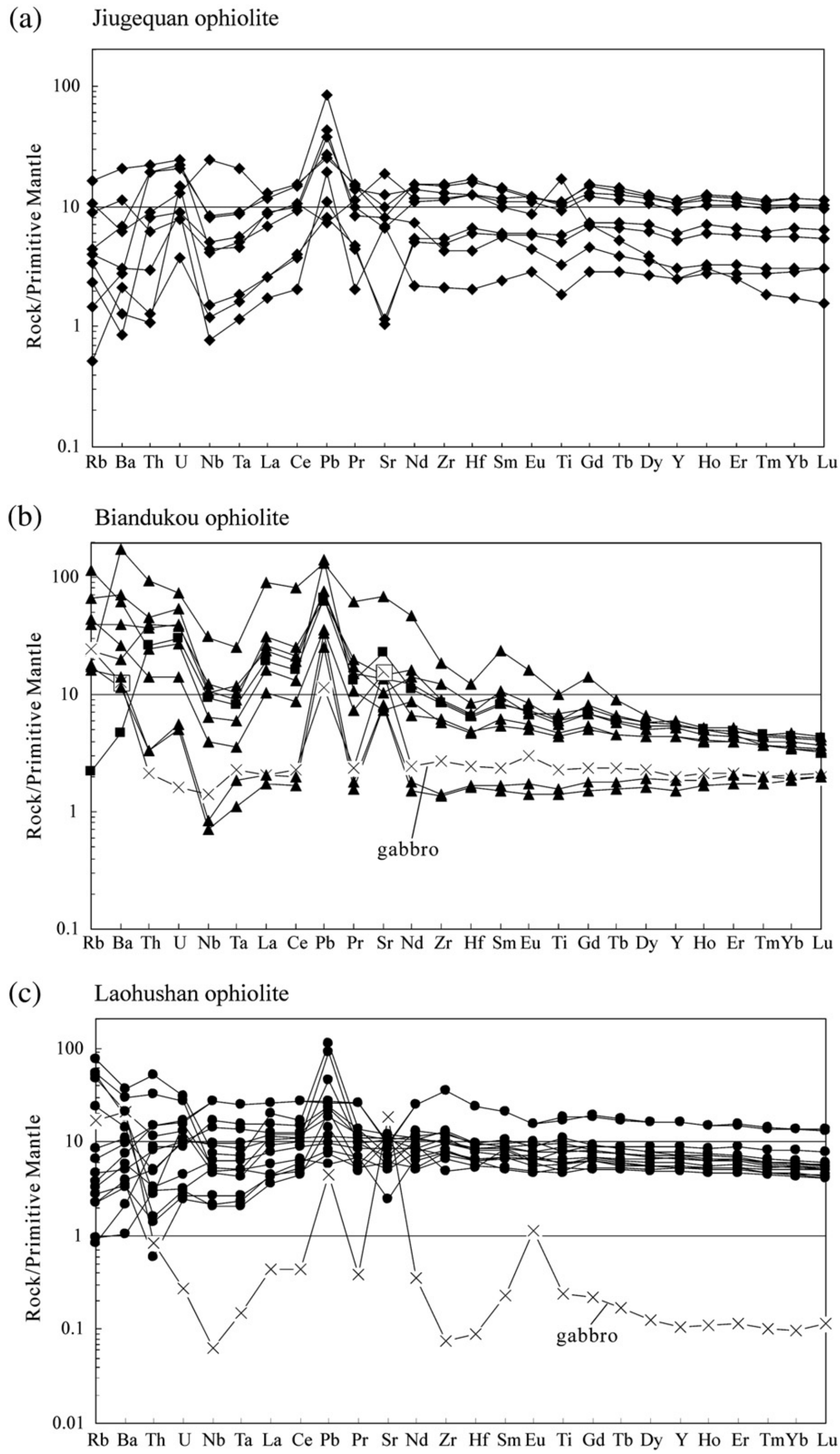

Fig. 10. Primitive mantle normalized spidergrams for ophiolite suites from the North Ophiolite Belt.

diagram (Fig. 16a), the lower tholeiite group plots in the basalt region and the upper boninite group ranges from basalt to andesite.

In comparison with the lower tholeiite group, all samples (including pillow lavas and dolerite dykes) of the upper group have lower HFSEs and REEs, and higher Cr, Co and Ni. In Zr–Zr/Y, Ti–V, and Y–Cr discriminant diagrams (Fig. 16b–d), the doleritic and gabbroic samples in the lower tholeiite group display a predominant MORB affinity, whereas the upper group samples plot nearly all in the boninite field.

Zircon U–Pb dating reveals that the boninite complex becomes younger from the lower tholeiite group to the upper boninite group. Two gabbro samples from the lowest, and upper part of the tholeiite group and one gabbro sample from the lower part of boninite group gave zircon SHRIMP weighted mean age of 517 ± 4 Ma , 505 ± 8 Ma

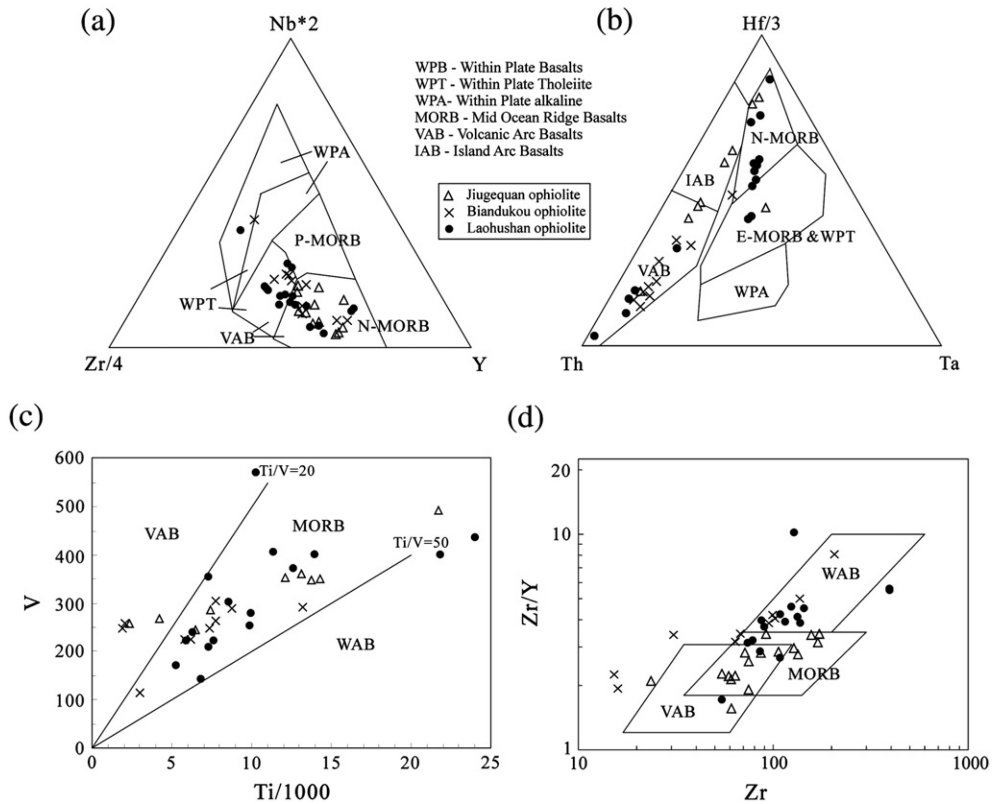

Fig. 11. Discrimination diagrams for basaltic rocks from the North Ophiolite Belt.

and 483 ± 9 Ma, respectively (Meng et al., 2010; Xia et al., in press) (see Fig. 14 for sample localities). These ages suggest a long erupted history in the forearc setting, and the later age is consistent with the Jiugequan SSZ-type ophiolite.

4.2. Arc volcanic rocks

The arc-volcanic complex, together with associated granite plutons, is the major component and occupies ~50–60% outcrop of the orogenic belt. This complex occurs continuously as a belt along the ~1000-km-long North Qilian oceanic suture zone. Continental collision juxtaposed the arc-volcanic sequence in parallel with belts of high-pressure metamorphic rocks and ophiolitic complexes. The arc-volcanic complex consists mainly of felsic to mafic volcanic rocks with minor shoshonite. These rocks, however, are poorly dated, and their tectonic significance has been debated for a long time (e.g., Xu et al., 1994; Xia et al., 1995a, 1995b; Wang et al., 2005). This volcanic sequence is also of particular interest in being the major host rocks of Cu–Pb–Zn sulfide mineralization, e.g., the Baiyin massive Cu–Pb–Zn sulfide deposit, which is the largest of its kind in China (Bian, 1989; Peng et al. 1995).

4.2.1. Arc-volcanic rocks in Qilian region

As shown in Fig. 2, the volcanic complex in the Qilian region extends between the two ophiolite belts along the major tectonic WNW-trending of the orogenic belt. This complex is intruded by the Qaidano granite pluton in the west and juxtaposes in parallel with three slices of high-pressure metamorphic rock assemblage including high-grade blueschist and eclogite, which suggests that exhumation of the HP rocks might be related to the arc-continent collision.

The volcanic complex is comprised predominantly of felsic (dacite to rhyolite) rocks with minor intermediate to mafic rocks. Most of the rocks have undergone greenschict-facies metamorphism and deformation with a penetrative foliation. Xia et al. (1995a, 1995b) interpreted the volcanic rocks as a bimodal basalt–rhyolite suite formed in a Neoproterozoic continental rift on the basis of questionable Rb–Sr isotopic dating.

Major element analyses show that compositions of volcanic rocks in the Qilian Region are actually intermediate to acid with variable SiO_2 (55–82 wt.%) and low TiO_2 (0.1–0.6 wt.%) and plot consecutively from basaltic andesite, andesite, dacite to rhyolite in the TAS diagram (Fig. 17a). In the AFM diagram (Fig. 17b), all samples display a calc-alkaline magmatic series. Two volcanic groups, i.e., the sodium-rich group and potassium-rich group, have been distinguished. The sodium-rich volcanic rocks have high Na_2O (3.0–7.4 wt.%) and Na_2O/K_2O ratios (1.6–83), but relatively low concentrations of LILE and LREE. They show rather flat chondrite-normalized REE patterns with weak or no Eu and Sr anomaly. The potassium-rich volcanic rocks, in contrast, have low Na_2O (0.15 − 2.72 wt.%), low Na_2O/K_2O ratios (0.05–0.92), high concentrations of LILEs and Th, U, Pb, but low Sr and Ti and show LREE enriched patterns with a negative Eu anomaly.

Zhang et al. (1997a, 1997b) reported single-zircon TIMS ages of 466–481 Ma for a felsic volcanic rock. The sample (09QL73) used for zircon U–Pb dating is a deformed rhyolite with porphyroblastic quartz and feldspar. Zircons are colorless and euhedral with the long axis varying from 100 to 200 μm and length/width ratios from 1.2 to 2. They all display oscillatory bands of magmatic origin in CL images. LA-ICPMS analysis gives relatively uniform U (417–956 ppm) and Th (343–900 ppm) and Th/U ratios (0.52–1.39). Seventeen analyses of zircons yield $^{206}Pb/^{238}U$ ages of 479–511 Ma with a weighted mean of 494 ± 6 Ma (MSWD = 0.84; Fig. 18).

4.2.2. Arc-volcanic rocks in Baiyin region

The Baiyin region is located in the eastern end of the North Qilian orogenic belt. Volcanic rocks in this region outcrop over an area of ~40 km^2. As the major host of the large Cu–Pb–Zn sulfide mineralization field, these rocks have been extensively studied for their

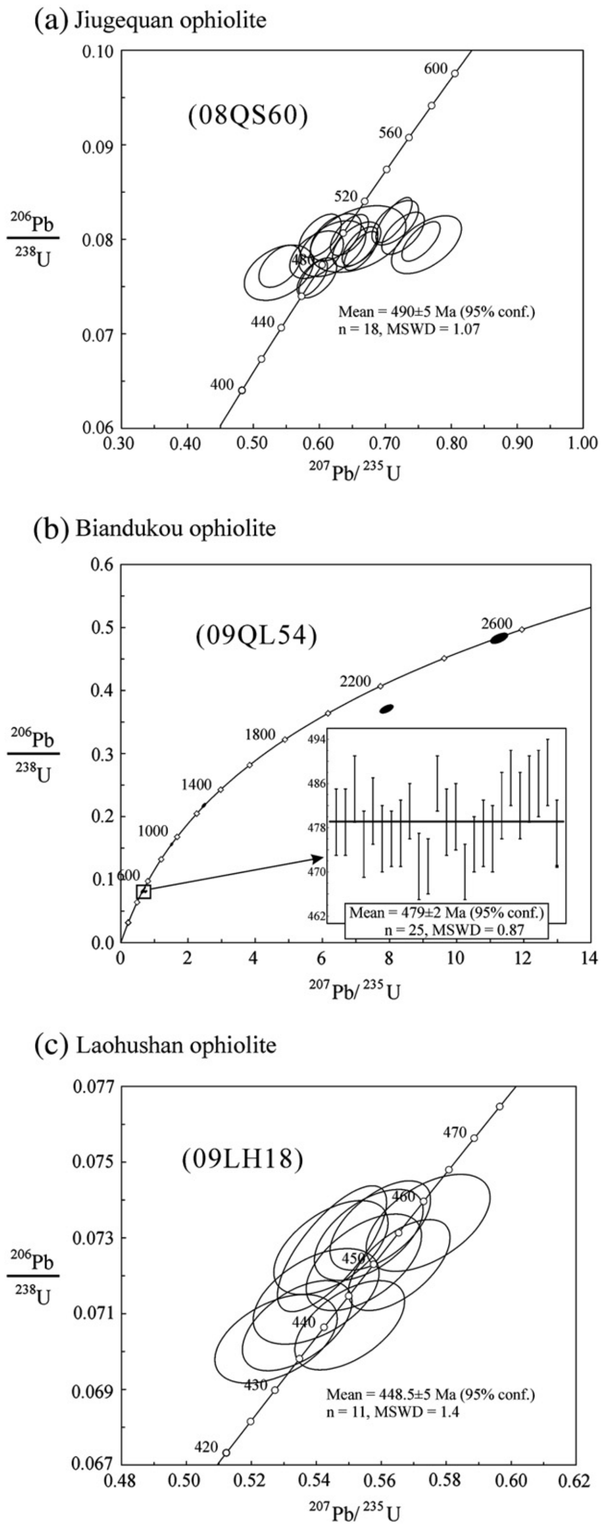

Fig. 12. Concordant diagrams for zircon SHRIMP analyses from gabbroic samples in the North Ophiolite Belt.

petrology, geochemistry, forming ages and tectonic settings (see Wang et al., 2005 and references therein).

As described in details by Wang et al. (2005), the lithologies of the Baiyin volcanic rocks are predominantly felsic and minor mafic, including rhyolitic and basaltic lavas and pyroclastic rocks. They occur as deformed tectonic slices, separated by WNW-trending ductile shear zones along which the rocks have been mylonitized. Most of the rocks have a penetrative foliation that strikes 120°–130° and dips 50°–70° S. The volcanic rocks are unconformably overlain by a metasedimentary sequence composed chiefly of phyllite and marble with some intercalated beds of Fe–Mn nodules and carbonaceous shale. Pb–Zn–Cu sulfide deposits mainly occur in the felsic volcanic rocks.

The Baiyin volcanic rocks display a bimodal pattern with mafic unit (SiO_2 46.5–57.5 wt.%) and felsic unit (SiO_2 69.1–82.0 wt.%) in the TAS diagram (Fig. 17a), and both mafic and felsic rocks exhibit a calc-alkaline trend in the AFM diagram (Fig. 17b). All mafic volcanic rocks are characterized by LREE enriched patterns with high (La_N/Yb_N) (2.8–8.1), Th/Nb (0.75–2.60), Th/La (0.30–0.87), and La/Nb (2.0–3.0) ratios, resembling volcanic arc basalts in the present-day supra-subduction zone environment (e.g., Pearce and Norry, 1979). The felsic volcanic rocks can also be subdivided into high-Na (Na/K > 1) and high-K (Na/K < 1) groups, as are volcanic rocks in the Qilian region (see earlier discussion). They display strong supra-subduction zone signature with negative Nb, Sr, Ti anomalies and relatively high Th/Nb ratios (0.8–1.6). The mafic volcanic rocks have ($^{87}Sr/^{86}Sr$)$_i$ ratios of 0.7064 to 0.7067 and $\varepsilon_{Nd(T)}$ values of −1.4 to +3.1, whereas the felsic volcanic rocks have ($^{87}Sr/^{86}Sr$)$_i$ ratios of 0.7046 to 0.7061 and $\varepsilon_{Nd(T)}$ values of +4.4 to +7.7. The Sr–Nd isotopic data suggest that the Baiyin volcanic rocks most probably formed in an island arc environment through partial melting of mafic rocks from a depleted source rather than from the anatexis of continental crust (Wang et al., 2005).

Xia et al. (1996) reported Sm–Nd and Rb–Sr isochron ages of the rocks ranging from 1292 ± 69 Ma to 522 ± 44 Ma for the mafic volcanic rocks and 606 ± 3 Ma for the felsic volcanic rocks, and therefore they concluded that the bimodal volcanic rocks formed in a Precambrian continental rift. Reliable zircon U–Pb ages by SHRIMP and LA-ICPMS reported in recent years are 446 ± 3 Ma and 467 ± 2 Ma for felsic volcanic rocks (Wang et al., 2005; He et al., 2006), 465 ± 4 Ma for a mafic volcanic rock (Li et al., 2009a, 2009b), which should represent the forming ages of the Baiyin island-arc volcanic rocks.

4.3. Granite/granodiorite plutons

Most granite/granodiorite plutons occur as elongated bodies within the island-arc igneous belt and the joint area between the North Qilian orogenic belt and the Alashan block. Their long axes extend along major tectonic line of the Qilian Orogen. The bulk volume of the plutons is much smaller than granitic pluton belts of Gangdese in Tibet and Andes in South America. On the basis of forming ages, these granite/granodiorite plutons can be subdivided into (1) volcanic arc granite (VAG) (520–460 Ma), (2) syn-collisional granite (440–420 Ma) and (3) post-collisional granite (<400 Ma). Most young plutons (<440 Ma) occur in the north. Adakitic plutons with U–Pb zircon ages of 438–450 Ma are also reported in the west and east part of the orogenic belt (Tseng et al., 2009; Chen et al., in press). Fig. 19 shows the distribution and ages of granitoid plutons in the North Qilian orogenic belt.

4.3.1. VAG plutons

The VAG plutons occur as individual intrusions within the arc igneous belt and the northern ophiolite belt all along the North Qilian orogen (Fig. 2). These plutons are variable in size and some large ones are usually lithologically compound with rock assemblage of gabbro, diorite, granodiorite and granite. Geochronological studies revealed that they formed in the epoch of oceanic subduction from ~520 Ma to 460 Ma (Mao et al., 2000; Song et al., 2004a, 2004b, 2004c; Wu et al., 2004, 2006, 2010; this study). Some large intrusions have been well documented, including (1) Kekeli diorite-granodiorite intrusion (476–512 Ma, Wu et al., 2010), (2) Chaidanuo biotite monzonitic granite intrusion (508–516 Ma, Wu et al., 2010; this study), (3) Niuxinshan quartz-diorite intrusion (477 Ma Wu et al., 2006,

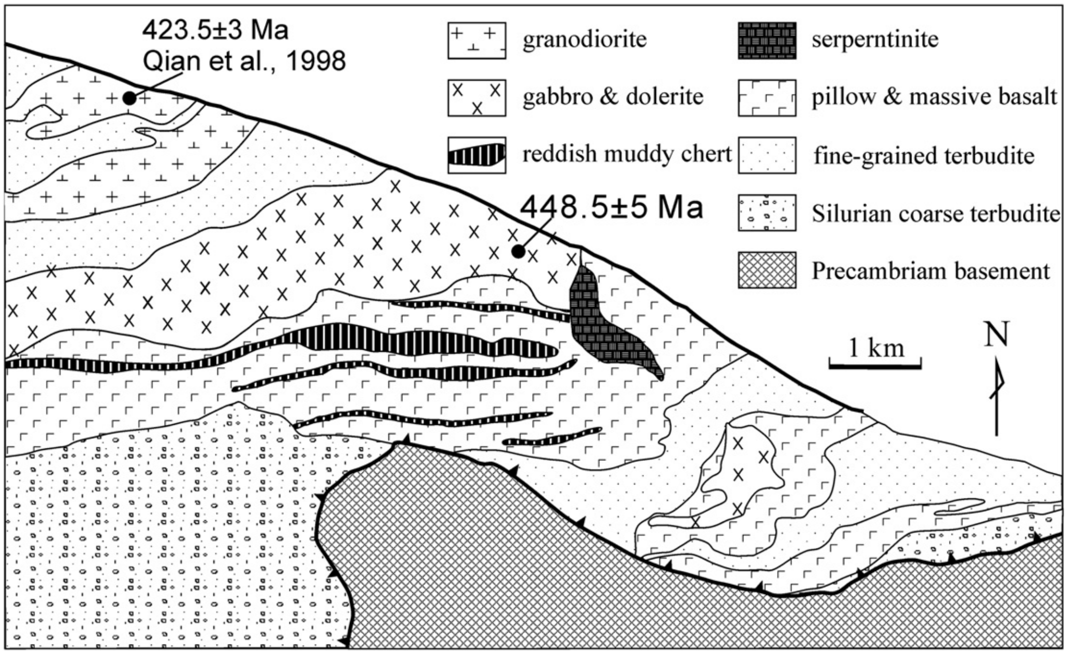

Fig. 13. Geological map of the Laohushan ophiolite (modified after Qian et al., 2001).

2010), and (4) The Leigongshan adakite–granodiorite intrusion (453 Ma, Tseng et al., 2009).

The Kekeli diorite–granodiorite intrusion crops out in the south margin of the Qilian orogen. It is an I-type pluton with mineral assemblage of Amp + Pl + Kfs + Qtz. Mafic magmatic enclaves (MME) are well preserved within the intrusion. This intrusion is chemically characterized by low SiO_2, high CaO and total Fe_2O_3 and metaluminous with an alumina saturation index [Al/(Ca − 1.67P + Na + K)] of less than 1.0. U–Pb SHRIMP dating for zircons from two samples suggests that it is a multi-stage intrusion with ages ranging from 512 Ma to 476 Ma (Wu et al., 2010).

The Chaidanuo intrusion is an elongate body (~60 km long and ~8 km wide), extending along the tectonic line within the arc igneous belt (Fig. 18). The intrusion is bounded by ductile fault in the northern margin and covered by Cenozoic sediments in the southern margin. Lithologies of this intrusion are predominantly granitic ranging from granodiorite to monzonitic granite. Some minor mafic bodies including gabbro and diorite also occur within this intrusion. The mineral assemblage of the granite consists of Pl + Kfs + Qtz + Bi and accessory phases such as zircon, apatite and titanite. All the analyzed samples from the main rock type of the Chaidanuo intrusion have low contents of MgO, FeO and CaO and plot in the granodioritic and granitic field. They are all peraluminous with an alumina saturation index of greater than 1.0 (1.03–1.28). In the Chondrite-normalized REE and Primitive mantle-normalized multi-element diagrams, all samples display strong negative anomaly of Eu, Ba, Sr and HFSEs (Nb, Ta and Ti). $(^{87}Sr/^{86}Sr)^t_S$, $[^{143}Nd/^{144}Nd]^t_S$ and $\varepsilon_{Nd}(t)$ are 0.7372–0.7473, 0.511692–0.511641 and −5.7 to −6.7, respectively (Wu et al., 2010). These features suggest that the Chaidanuo intrusion is typical S-type granite that was originated from partial melting of crustal

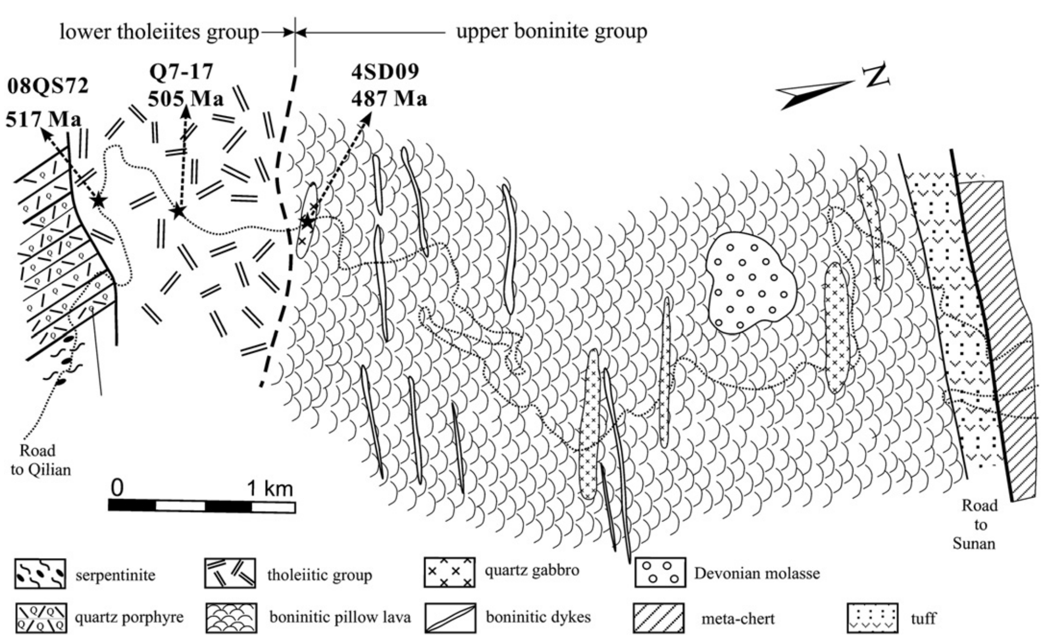

Fig. 14. Geological map and cross-section of the Dachadaban boninite complex.

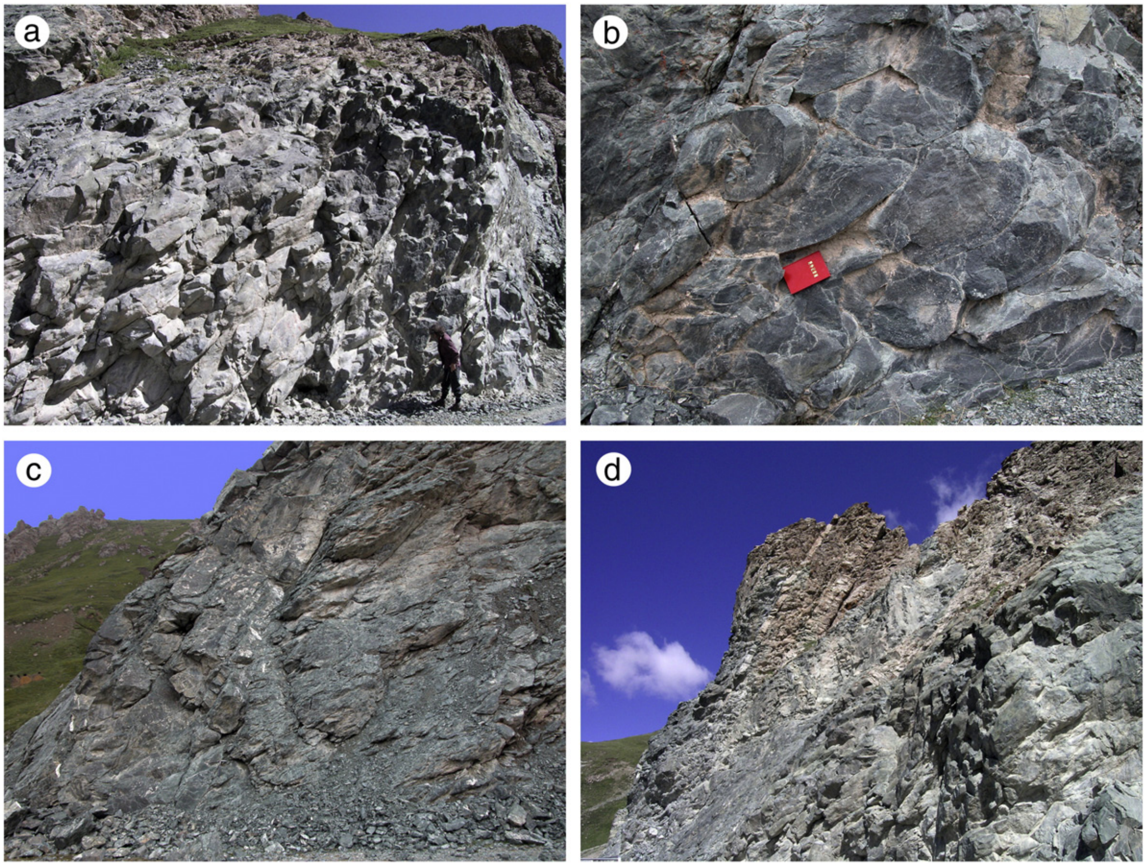

Fig. 15. Photographs showing the boninite complex. (a) and (b) boninitic pillow lava. (c) and (d) boninitic dykes intruded in boninitic pillow lava.

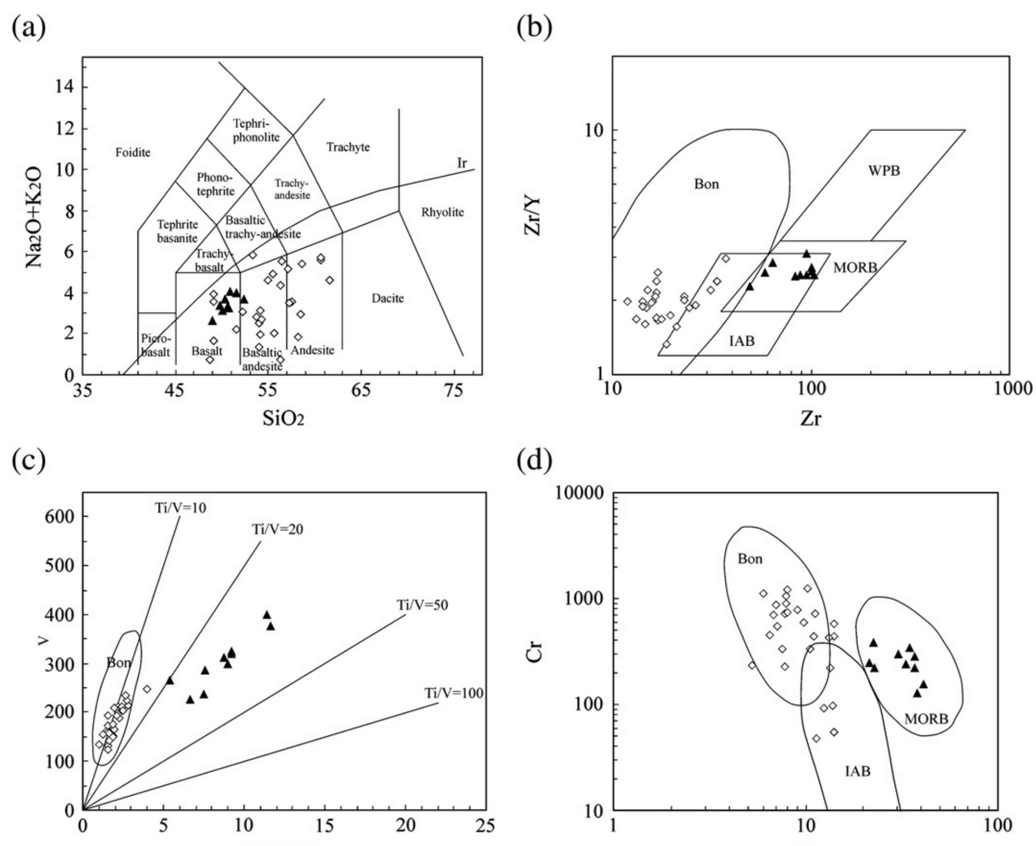

Fig. 16. TAS (a), Zr–Zr/Y (b), and TiO_2–V (c) Y–Cr (d) discriminant diagrams for the Dachadaban boninite complex. MORB, mid-ocean ridge basalts; IAB, island arc basalts; WPB, within plate basalts; Bon, boninites. See Pearce (2003) for further references to these discriminant diagrams.

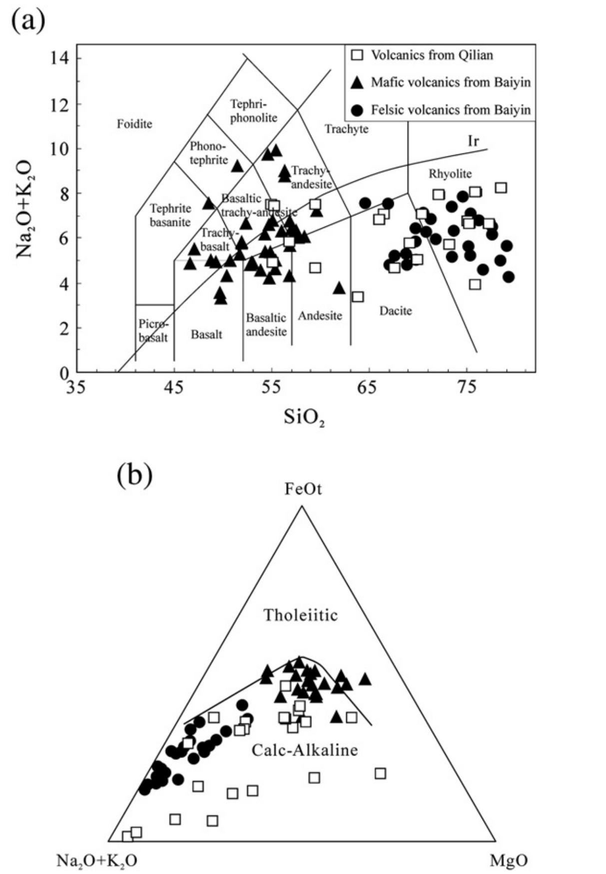

Fig. 17. Total Alkalis (Na_2O+K_2O) versus SiO_2 plot of the volcanic rocks in Qilian Region.

materials with plagioclase as a residual phase or a large scale of crustal assimilation. Wu et al. (2010) reported a zircon U–Pb age of 508 ± 5 Ma by SHRIMP for the Chaidanuo intrusive complex. Zircons from our sample, however, yielded very complicated results with detrital zircon ages of 954–743 Ma and magmatic zircon ages of 516 ± 4 Ma (Chen et al., unpublished data). Therefore, we can conclude that the Chaidanuo intrusive complex was formed at ca. 508–516 Ma through partial melting of a juvenile crust. This intrusion records the oldest arc magmatic activity in the North Qilian orogenic belt.

The Niuxinshan intrusion, located south of the town of Qilian, is lentoid and occupies over an area of ~110 km^2. This intrusion mainly

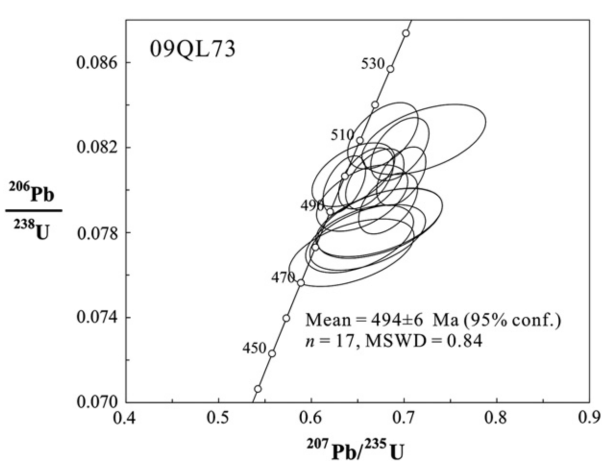

Fig. 18. Concordia diagram for zircon U–Pb LA-ICPMS analyses for the volcanic sample 09QL73 in Qingshuigou, Qilian.

consists of reddish granite with mineral assemblage of Pl + Kfs + Qtz with minor Hb, Bi, apatite, sphene and zircon and is intruded by late quartz-diorite. Zircon U–Pb analyses by SHRIMP gave ages of 477 ± 7 Ma for the reddish granite (Wu et al., 2006).

4.3.2. Syn-collisional pluton

Two syn-collisional plutons that occur in the northern margin of the orogen have been recognized. They were formed in the period of continental collision following the complete ocean basin closing and seafloor consumption.

The Jinfosi intrusion crops out as a lentoid body (~60 km long and 10–12 km wide, over an area of ~620 km^2), and extends in NW-direction in the northwesten part of the North Qilian orogenic belt. It intruded the Ordovician back-arc basin volcanic complex and Silurian sedimentary sequence. This intrusion consists predominantly of quartz monzonite and monzonitic granite with minor quartz diorite and granodiorite. Mineral assemblage of quartz, microperthitic microcline, plagioclase, biotite, muscovite, tourmaline, garnet, apatite and zircon indicates S-type affinity. Whole-rock analyses show all samples are peraluminous with a molecular ratio $Al_2O_3/(CaO+Na_2O+K_2O)$ of 1.01–1.25, and have clear negative anomalies of Eu, Sr, Ba, Nb, Ta and Ti in the primitive mantle-normalized multi-element diagram (Zhang et al., 1995; Hu et al., 2006; Wu et al., 2010).

Zhang et al. (1995) reported whole-rock Rb–Sr isochron ages of 404–419 Ma. Zircon U–Pb analyses by SHRIMP yielded a weighted mean age of 424 ± 3 Ma (Wu et al., 2010). The forming ages of the Jinfosi intrusion is much later than arc volcanic rocks (~500–440 Ma), VAG intrusions (520–460 Ma) and high-pressure metamorphic rocks (see later discussion), but the same as ultrahigh-pressure metamorphism associated with continental deep subduction in the North Qaidam UHP belt (e.g. Song et al., 2005, 2006).

The Laohushan intrusion is located in the eastern part of the North Qilian orogenic belt and intrudes the Laohushan ophiolite and sedimentary sequence. It is an elongate body (~2 × 20 km^2) and consists of quartz diorite, pyroxene diorite, tonalite and minor quartz monzonite. Zircon U–Pb analyses by TIMS yielded an age of 423.5 ± 3 Ma (Qian et al., 1998).

4.3.3. Post-collisional intrusion

The post-collisional intrusions were recognized in Wuwei-Jinchuan region, the joint area between the North Qilian orogenic belt and the Alashan block (Fig. 18). Lithologies in these intrusions are chiefly quartz-monzonitic and granitic with $Al_2O_3/(CaO+Na_2O+K_2O)$ molecular ratios of 1.0–1.1. Rock forming minerals are plagioclase (An 15–28), microperthitic microcline, quartz and biotite with accessory minerals including apatite, sphene, magnetite-ilmenite and zircon. Zircon U–Pb analyses by LA-ICP-MS yielded 374–403 Ma (Wu et al., 2004; Hu et al., 2005).

5. High-pressure low-temperature metamorphic rocks

Two sub-belts of high-pressure metamorphic (HPM) rocks are readily identified in the North Qilian suture zone (Wu et al., 1993; Song, 1997): (1) a low-grade blueschist belt with a typical assemblage of Lws + Pmp + Gln ± Arg, and (2) a high-grade blueschist belt with an assemblage of Grt + Phn + Gln + Ep that locally encloses massive blocks of eclogite, meta-chert, serpentinite and marble. On the basis of petrological, mineralogical and geochronological studies, this belt was suggested to be one of the oldest "cold" oceanic subduction zones with a thermal gradient of ~6–7 °C/km on Earth. Song et al. (2009a, 2009b, 2009c) have reviewed these HPM rocks in details on rock types, mineral assemblages and composition, metamorphic ages and the P-T-t path.

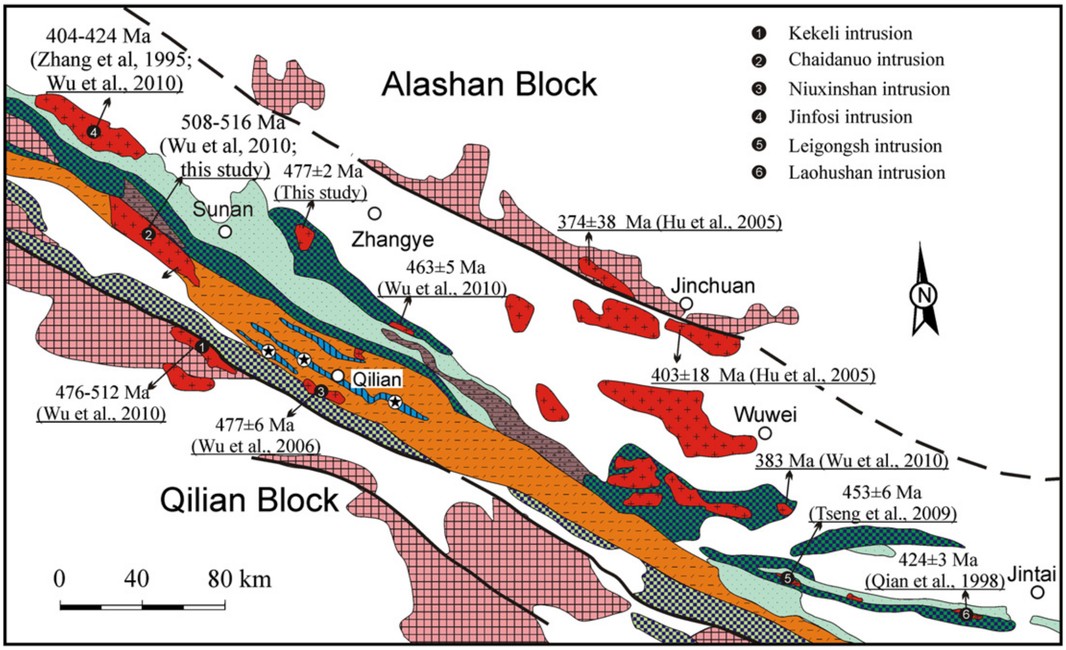

Fig. 19. Geological map showing major granitic plutons and their ages.

5.1. Low-grade blueschist belt

The NW-trending low-grade blueschist belt of ~200–500 m wide extends for ~20 km along the Bailong River, ca. 20 km southwest of the town of Sunan (Wu et al., 1990). It is thrust southwestwards onto the Devonian molasse to the south. To the further south is a large granitic pluton in parallel with the low-grade blueschist belt. To the north of the low-grade blueschist belt is an ophiolitic complex comprised of blocks of serpentinized peridotite, gabbros, pillow lavas and diabasic dykes with thin-layers of radiolarian chert. Copper mineralization is widespread within this ophiolitic complex.

Blueschists along the Bailong River are strongly deformed with isoclinal folds and intense foliation on both macro and micro scales. The intensity of deformation decreases gradually northeastwards into non-deformed glaucophane-bearing meta-basalt. Protoliths of low-grade blueschists are mainly basaltic rocks with minor felsic ones. The low-grade blueschists are characterized by high-pressure metamorphic (HPM) assemblages of Lws + Gln + Pmp + Ab + Arg, Lws + Chl + Ab, and Pmp + Gln + Chl + Ab + Arg, which best constrain P–T conditions for the low-grade blueschist at ~250–350 °C and 0.6–1.1 GPa (Song et al., 2009a). P–T pseudosection calculation shows that the metamorphic P–T conditions for low-grade blueschist are limited in the range of 320–375 °C and 0.75–0.95 GPa (Zhang et al., 2009). The variation of mineral assemblages may suggest pressure decrease from southwest to northeast.

Chemical analyses show that the protoliths are sub-alkaline tholeiitic basalt with SiO_2<50 wt.%, TiO_2 1.12–1.49 wt.%, and relatively high MgO (7.0–9.6 wt.%) and low to medium K_2O content (0.16–1.1 wt.%). In the primitive mantle normalized (Sun and McDonough, 1989) multi-element diagram, these three rocks show patterns consistent with N-type MORB except for the enrichment of fluid-mobile LILEs such as Cs, Rb, Ba, U and to a lesser extent Th. In trace element discrimination diagrams, they all plot in the N-type MORB field (Song et al., 2009a).

5.2. High-grade blueschist belt

The high-grade blueschist belt of about 140 km long occurs tectonically as three NW-trending slices within arc-type siliceous volcanic rocks (Fig. 2). These slices are composed of typical subduction-zone mélange with various blueschist- to eclogite-facies metamorphosed blocks and lenses of limestone and ophiolitic fragments, including serpentinite, basalt, pelite and pelagic chert within a blueschist-facies meta-greywacke matrix.

5.2.1. Meta-greywackes and olistostrome

The meta-greywacke matrix of the mélange is characteristic of accretionary wedge rock assemblage and constitutes the major components of the high-grade blueschist belt (Wu et al., 1993; Song, 1997). Meta-greywackes are foliated, and contain a blueschist-facies mineral assemblage of Gln + Phn + Pg + Ep + Ab + Qtz ± Grt. A ~100-m-thick layer of conglomerate with miscellaneous gravels occurs in the southern border of Slice A in Qingshuigou cross-section and extends for about 5–8 km. Song (1996) interpreted it as an “olistostrome” deposit. The olistoliths contain varying-size, strongly deformed blocks of marble, meta-chert, serpentinites, and mafic and siliceous volcanic rocks within a greywacke matrix.

Blueschist- to eclogite-facies metamorphosed turbidites are also recognized in the high-grade blueschist belt, and show deformed, interbedded structures with thicker, light-colored layers of meta-sandstone and thinner, dark-colored layers of meta-pelite (blueschist). The meta-sandstone has a mineral assemblage of Grt + Phn + Qtz ± Gln ± Ep.

5.2.2. Eclogite and mafic blueschist

Eclogites in the North Qilian orogenic belt were first reported and studied in details by Wu et al. (1993). All eclogites (including mafic blueschists) occur as blocks or lenses of varying size within felsic blueschists. The eclogite blocks are mainly found in slices of the high-grade blueschist belt (Fig. 2). In terms of mineral assemblages, these eclogites can be grouped into two types (Song et al., 2007): (1) phengite-rich eclogite with a peak-stage Grt + Omp + Phn + Rt assemblage plus minor epidote, and (2) epidote-rich eclogite with a Grt + Omp + Ep/Cz + Gln + Rt ± Qtz assemblage and minor phengite and paragonite. Most epidote eclogites are strongly deformed, and show mineral (epidote/clinozoisite, omphacite and phengitic mica etc.) alignment along the foliation overprinting the undeformed assemblage. Mineral compositions and oxygen fugacity vary systematically with the strength of deformation (Cao et al., 2011). Most eclogite blocks have undergone retrograde blueschist-facies overprinting; some are completely retrograded into mafic blueschist.

Inclusions of lawsonite and lawsonite pseudomorphs are present in some porphyroblastic garnets in both eclogite types (Zhang and Meng, 2006, Song et al., 2007; Zhang et al., 2007). Lawsonite pseudomorphs show rectangular and triangular shapes and consist of aggregates of Cz + Pg ± Phn ± Omp defining a reaction relationship of Lws + Jd (Omp) = Cz + Pg + H_2O. The numerous lawsonite pseudomorphs together with omphacite inclusions in garnet suggest that lawsonite was ubiquitous during the peak stage of eclogite-facies metamorphism associated with "cold" oceanic subduction. P–T calculations give a temperature range of 460–550 °C and a pressure range of 2.20–2.60 GPa, which lie mainly in the lawsonite-eclogite field (Song et al., 2004b, 2007; Zhang et al., 2007; Wei et al., 2009).

On the basis of mineral assemblage and geochemical analyses, protoliths of eclogites can be subdivided into three groups, (1) high-K basaltic group (phengite-rich eclogite), (2) low-K basaltic group and (3) gabbroic group. The high-K eclogite samples have variable SiO_2 from 44 to 55 wt.%, relatively high K_2O (K_2O > 2.0 wt.%), high but variable TiO_2 (1.15–2.98 wt.%) and most samples plot in the alkaline fields of tephrite basanite, trachybasalt and basaltic trachyandesite in the TAS diagram. Trace elements indicate that phengite eclogites have characteristics of present-day E-type MORB and ocean island basalts (OIB). The low-K group eclogites, in contrast, are sub-alkaline basalts and show N- to E-type MORB affinities. The gabbroic group is characterized by low concentrations of REEs and HFSEs and positive Sr and Eu anomalies.

5.2.3. Eclogite-facies metapelites

Most metapelites occur as country rocks or are interlayered with eclogites. Song et al. (2007) reported two kinds of pelitic schist on the basis of their different mineral assemblages. (1) Carpholite-bearing chloritoid-glaucophane schists with assemblage of Grt + Car + Cld + Phn + Rt + Qtz (±Gln) and (2) Grt-Omp-Phn-Gln schist. Wei and Song (2008) reported talc in the Chloritoid-glaucophane schists.

Mg-carpholite, an important index mineral of high-H_2O phase in the cold subduction zone, has been found so far in meta-pelite from the southern part of the Baijingsi cross-section, 30 km east of the town of Qilian. The Car-Cld schist mainly consists of Mg-carpholite (15–20%), garnet (~5–8%), Mg-rich chloritoid (~10–15%), phengite (10–15%) and quartz (30–40%) with minor tourmaline. Rare glaucophane grains occur in the matrix, or as inclusions in garnet. Coarse-grained prismatic Mg-carpholite crystals of 0.1 − 0.4 mm occur in the matrix, and as small inclusions in chloritoid. Mg-rich chloritoid ($Mg/[Mg + Fe^{2+}] = 0.46 - 0.55$) occurs as porphyroblastic crystals in equilibrium with Mg-carpholite, garnet and phengite.

Mg-carpholite is characterized by high MgO, low FeO and extremely low MnO with X_{Mg} [$= Mg/(Mg + Fe^{2+} + Mn)$] ranging from 0.73 to 0.87, X_{Fe} from 0.13 to 0.27, and X_{Mn} from 0.000 to 0.002. THERMOCALC (Powell et al., 1998) calculation gives equilibrium T = 520–530 °C and P = 2.45–2.50 GPa for carpholite-bearing schists (Song et al., 2007; Yu et al., 2009).

The Grt-Omp-Phn-Gln schist occurs as a ~100 m thick layer in the Baijingsi cross-section and is bounded by a large block of eclogite to the north and the Car-Cld schist to the south (Fig. 6b). This schist consists of garnet porphyroblasts set in a foliated fine-grained matrix of omphacite, phengite, glaucophane, rutile, epidote and quartz. The Grt-Omp-Phn geothermobarometer of Ravna and Terry (2004) gives equilibrium T = 445–496 °C and P = 2.15–2.25 GPa (Song et al., 2007).

5.2.4. Meta-chert

Meta-cherts occur as blocks or layers (~50 m in maximum thickness) enclosed in meta-greywacke and pelitic schists. Most meta-cherts are strongly deformed with isoclinal folds. They are dominated by elongate recrystallized quartz with minor phengitic mica; some samples also contain minor garnet and glaucophane. Mn ores have been minded in the manganese-bearing meta-chert, suggesting a protolith of pelagic sediment.

5.2.5. Marble

Marble also occurs as blocks of varying size in felsic blueschists. Some marble blocks have banded structure with inter-bedded layers of Cc + Qtz and Gln + Ep ± sodic Cpx (X_{Ae} = 0.61–0.79) assemblage.

5.3. High-pressure metamorphic ages

Geochronological studies of HPM rocks started in 1980s using K-Ar and $^{40}Ar–^{39}Ar$ methods on phengite and glaucophane for blueschists (Wu, 1987; Liou et al., 1989; Wu et al., 1993; Zhang et al., 1997a, 1997b; Liu et al., 2006). More recently, zircon U–Pb SHRIMP technique has been used to determine the metamorphic ages of eclogites (Song et al., 2004a, 2004b, 2004c, 2006; Zhang et al., 2007). The low-grade blueschists, on the other hand, have not been precisely dated so far.

Five eclogite samples from the North Qilian HPM belt have been dated using zircon SHRIMP method by Song et al. (2004a, 2004b, 2004c, 2006) and Zhang et al. (2007). They gave weighted mean ages from 463 ± 6 Ma to 489 ± 7 Ma for HPM and from 544 to 710 Ma for protoliths (Song et al., 2004a, 2004b, 2004c; Zhang et al., 2007). These HPM ages are statistically similar, but the mean differences of ~20 m.y., reflecting differences in the timing of eclogite-facies metamorphism in different eclogite blocks of the same HPM belt.

Histogram of all zircon analyses of four eclogite samples give metamorphic ages shown in Fig. 20. Four accumulate age peaks are 710–650, 544, 472 and 421 Ma. The old core ages of 710–650 Ma and ~544 Ma probably represent crust forming ages in the Qilian Ocean, although Zhang et al. (2007) interpreted the former ages as crustal contamination prior to subduction (Zhang et al., 2007). The peak at ~472 Ma is accumulated from metamorphic ages (463 to 489 Ma) of the four eclogite samples and represent the timing of eclogite-facies metamorphism. The age peak at ~421 Ma (404–424 Ma) is distinctive, is younger than the blueschist-facies metamorphism or cooling time of the HPM belt (see later discussion), but is consistent with the continental collision with mountain building (molasse formation) in the Late Silurian–Early Devonian time. Moreover, this age is also consistent with the UHPM and exhumation ages of the North Qaidam *continental-type* subduction zone inferred from dating of zircons from garnet peridotites and coesite-bearing meta-pelites (~430–400 Ma, Song et al., 2005, 2006).

Ar–Ar dating of phengitic mica from blueschists in the high-grade blueschist belt yields plateau ages of 448 ± 11 Ma (Liou et al., 1989), 446–454 Ma (Liu et al., 2006) and 450–489 Ma, which should represent the major blueschist-facies metamorphism. Some $^{40}Ar/^{39}Ar$ ages

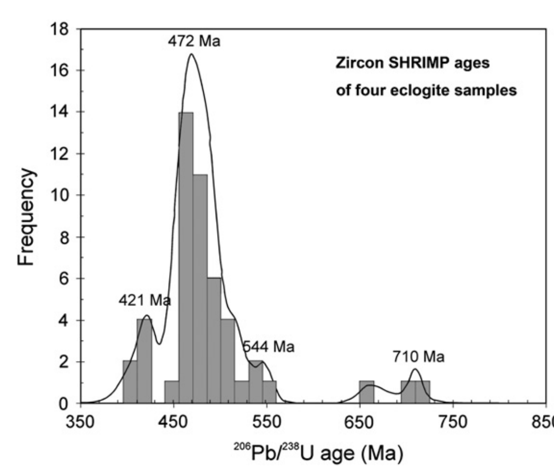

Fig. 20. Histogram of apparent $^{206}Pb/^{238}U$ age of all analyses (After Song et al., 2009a, 2009b and references therein).

of phengitic mica and glaucophane range from 420 to 400 Ma (Wu et al., 1993; Zhang et al., 1997a, 1997b) and most probably record the last exhumation event of the North Qilian HP belt corresponding to the orogenic uplift indicated by the deposition of the Early Devonian molasses.

Lin et al. (2010) reported Ar–Ar glaucophane ages of 415–417 from two lawsonite-bearing blueschist samples in the low-grade blueschist belt. This age is much younger than Ar–Ar ages of the high-grade blueschists, but is consistent with mountain building epoch from late Silurian to early Devonian (see following discussion).

6. Silurian flysch, Devonian molasse and post-Devonian covers

The Silurian flysch formation occurs as elongate belt in the north side the arc-volcanic magmatic belt along the North Qilian orogenic belt. Temporal and spatial distributions of the formation suggest that it may have developed in an Ordovician back-arc basin (Fig. 2), rather than a forearc basin as suggested by Yan et al. (2010). This formation consists predominantly of fine-grained siltstone and slate that forms a typical turbidite with Bouma sedimentary structures (Fig. 21 a–d). The coarse-grained, polymict conglomerate and sandstone mainly distribute on the two margins of the sedimentary basin, which represent under-water channel deposit. Gravels of conglomerates in the north are composed of granite, chert, sandstone, limestone and volcanic rocks, suggesting that they have sourced from the continent in the north, whereas gravels in the south are volcanic rock, chert and granite that soured from the volcanic arc. Zircon U–Pb dating for volcanic and granitoid clasts yielded ages of 515–429 Ma (Yan et al., 2010), consistent with ages of the volcanic arc and syn-collisional magmatism described earlier.

The Silurian flysch formation has deformed temporally in consistence with those Ordovician SSZ ophiolite; both are uncomformably

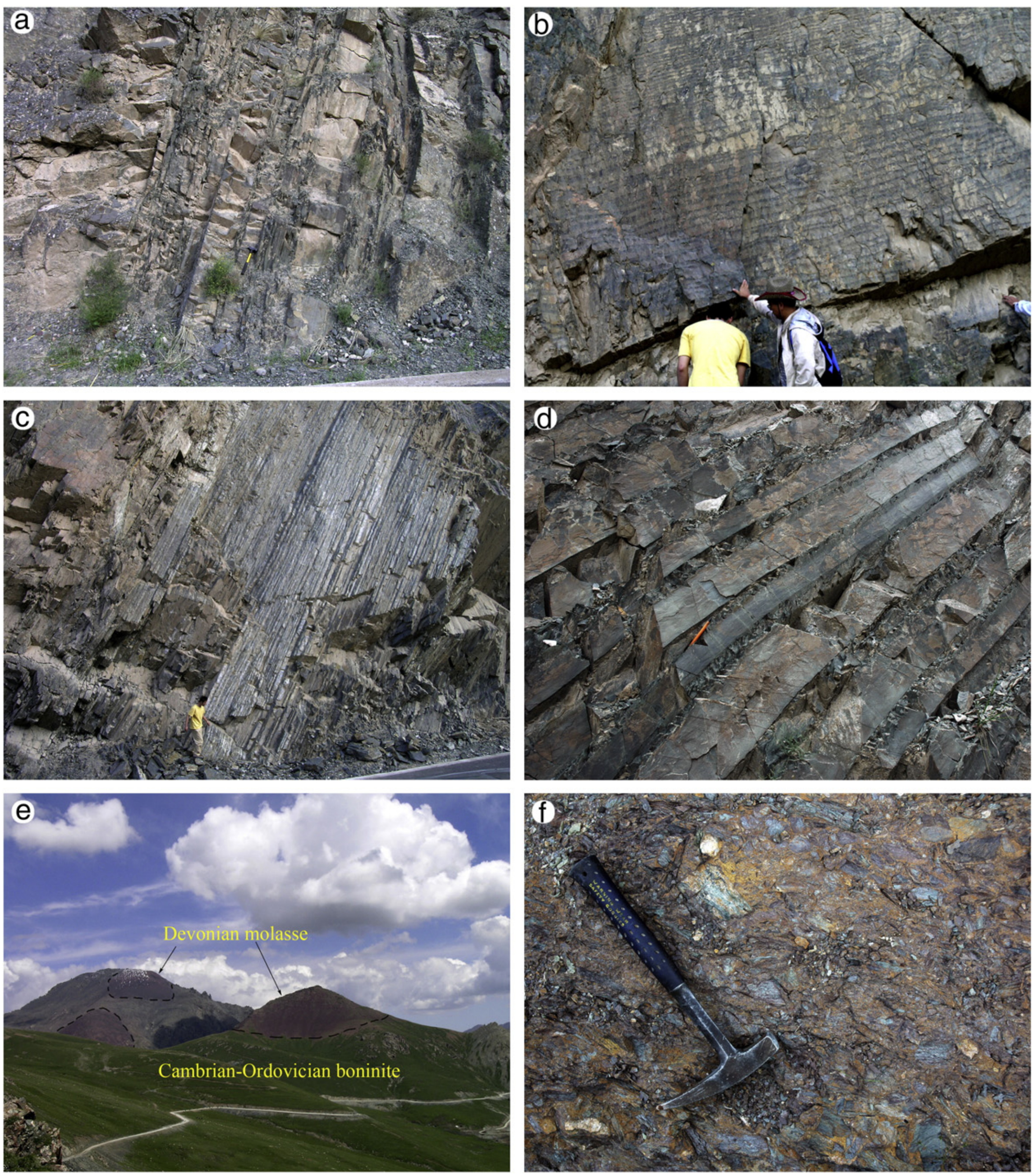

Fig. 21. Photographs showing Silurian flysh and Devonian molasse. (a) Coarse-grained, polymict conglomerate and sandstone in the Silurian flysh formation. (b)–(d) Fine-grained turbidites in the Silurian flysh formation. (e) Devonian molasse deposited on the Dachadaban boninitie complex. (f) Oligomictic conglomerate in the Devonian molasse.

covered by the Early Devonian molasse and stable-platform type sedimentary strata of late Devonian to Triassic eras.

The Early Devonian molasse distributes discontinuously in the North Qilian Mountains and lies unconformably over those early rock series, such as arc volcanic complex, ophiolites, HPM rocks and Silurian flysch formation. It mainly consists of poorly-rounded, non-sorting terrestrial conglomerates (Fig. 21e,f) and sandstones that in-situ deposit in an intermontane or foreland basin, which is interpreted as indicating mountain building processes (orogeny) in response to continental collision events.

The Late Paleozoic strata are stable epicontinental sedimentation changing from limestone to clastic rocks with coal layers that uncomformably cover the Silurian flysch and subduction complex.

7. Tectonic evolution of the Qilian Orogen

7.1. Breakup of supercontinent Rodinia and formation of the Qilian Ocean

Breakup of supercontinent Rodinia was thought to result from a mantle superplume activity in the Neoproterozoic (830–750 Ma) (e.g., Li et al., 2008 and references therein). All blocks on both sides of the North Qilian orogenic belt are believed to be fragments of Rodinia, because of wide-spread Neoproterozoic magmatic and metamorphic records (e.g., Wan et al., 2001; Lu, 2002; Li et al., 2005). Recognition of ~850 Ma CFBs as protoliths of eclogites in Yuka terrane, the North Qaidam UHP belt suggests that the onset of mantle superplume could be as early as 850 Ma (Song et al., 2010).

The early history of the Qilian Ocean (part of the Iapetus Ocean?) is little known, although it was supposed to start spreading at ~750 Ma as a result of Rodinia disintegration (e.g. Meert, 2003; Torsvik, 2003; Li et al., 2008). Some granitic intrusions with ages of 750–790 Ma in the Qilian orogenic belt and the Qilian block were interpreted to be products of continental rifting of Rodinia (Tseng et al., 2006; this study). The 530–560-Ma Yushigou ophiolite is the oldest one that has been recognized so far in the North Qilian orogenic belt. However, relic cores in zircons from some eclogite samples record ages of ~710 Ma; this age, despite being interpreted as crust contamination by Zhang et al. (2007), most probably represents the forming time of the early subducted ocean (gabbroic) crust. Therefore, it is reasonable to infer that seafloor spreading in the Qilian Ocean might have started at latest at ~710 Ma.

Some researchers suggested that the Qilian Ocean belongs to proto-Tethyan Ocean (e.g., Hou et al., 2006; Gehrels et al., 2011). However, the tectonic domain of Tethys, as originally defined, was referred to a ‘geosyncline’ that lay between the supercontinents of Laurasia and Gondwanaland (e.g. Sengör, 1984; Metcalfe, 1996). The Qilian Ocean, on the other hand, is associated with breakup of the Rodinia at ~750 Ma and closed at ~445 Ma, much older than the proto-Tethan Ocean. Therefore, the Qilian Ocean should be within the tectonic domain of Laurasia and temporally comparable with the Iapetus Ocean, a worldwide ocean that was opened in the Neoproterozoic as a consequence of break-up of supercontinent Rodinia, and closed and finally collided and formed the Appalachian orogenic belt in North America and the Caledonian orogenic belt in Europe in the Early Paleozoic (e.g., Van der Pluijm et al., 1990; McKerrow et al., 1991, 2000; Van der Voo, 1993; Torsvik et al., 1996; Niocaill et al., 1997; Snyder and Barber, 1997; Murphy et al., 2010).

7.2. Initiation of subduction of the Qilian Ocean

The initiation of lithosphere subduction is a hot issue that has been discussed for over a half century. Generally, the fundamental factor for subduction initiation is that a sufficiently cold and dense oceanic lithosphere is required so that the plate sinks spontaneously in the mantle under its own weight (e.g., McKenzie, 1977; Mueller and Phillips, 1991, Niu et al., 2003; Gurnis et al., 2004; Stern, 2004). Subducting slab as a result of its negative thermal buoyancy, further enhanced by changes to denser minerals with depth, is widely accepted as major driving force for plate motion (Niu et al., 2003 and references therein). Consider that under normal circumstances, a period of ~200 Myr is needed from the onset of lithosphere formation at an ocean ridge to its sufficiently cooled and thickened lithosphere to subduct along passive margins (e.g., Niu et al., 2003), the mature ocean basin would have been thousands of km wide (depending on plate-spreading rate) like the Atlantic Ocean before subduction initiation. Therefore, the onset of trench formation must be significantly later than an ocean basin opening. Critical evidence for the timing of subduction initiation, on the other hand, is always ambiguous in ancient orogenic belts, but can be inferred from (1) the earliest arc magmatism, (2) “infant arc” boninitic complex, and (3) HP/LT metamorphic rocks.

Determination of an “infant arc” in the Qilian orogenic belt is not straightforward. The maximum age of eclogite facies metamorphism in the Qilian orogenic belt is 489 ± 7 Ma (Zhang et al., 2007), much younger than arc magmatic ages (> 500 Ma) of granitic intrusions (Wu et al., 2010). Gabbroic samples in the lower tholeiitic part of the Dachadaban boninite massif gave zircon SHRIMP age of ~517 Ma (Xia et al., in press); this is the earliest magmatism in a fore-arc setting. We infer that subduction in the Qilian Ocean may be initiated at ~520 Ma, i.e., conversion of an Atlantic-type passive margin into an Andean-type active margin.

7.3. Development from Andean-type active margin (infant arc) to back-arc basin

Passive margin failure is the most accepted model of trench formation, for which the nucleation of subduction was thought to be as a direct consequence of the cooling of oceanic lithosphere, because the oldest (hence coldest and most dense) seafloor is adjacent to Atlantic-type continental passive margins (e.g., Mueller and Phillips, 1991), which can be further facilitated by sedimentary loading and water weakening (Erickson, 1993; Regenauer-Lieb et al., 2001). As oceanic lithosphere subducts, asthenosphere locally wells up and melts due to decompression (Stern, 2004), explaining the infant arc magmatism.

If the onset of “infant arc” in the Qilian Orogen began at ~520 Ma, the magmatic arc would be developed on an Andean-type continental active margin. The convincing evidence for this is the 516-Ma S-type Chaidano granitic intrusion. Geochemical analyses suggest this intrusion resulted from partial melting of continental crust as evidenced by a large number of inherited 750–900 Ma zircons of crustal materials representing a passive continental margin rifting by a mantle plume activity during Rodinia break-up. The 517–505 Ma MORB-like gabbro–dolerite complex in the lower part of the Dachadaban boninite complex also suggests the birth of an “infant arc” through upwelling of mantle during subduction initiation (Xia et al., in press). The magmatic sequence from the lower MORB-like tholeiites (lherzolite melts) to upper boninite (harzburgite melts) indicates increasing depletion of the mantle source with time and development of infant arc magmatism.

The earliest SSZ-type ophiolite in the Jiugequan region is 490 Ma, overlapping the formation time of boninite in the fore-arc setting, and represents extension of back-arc spreading center. This means a conversion from Andean-type active margin to Western Pacific-type trench–arc–back-arc-basin system may have occurred at ~490 Ma, while part of the continental margin (fore-arc) splitted from the mainland through back-arc extension. The latest ophiolite of 448.5 ± 5 Ma in the Laohushan region is consistent with the minimum ages of arc volcanic rocks in the Baiying region and Ar–Ar ages of blueschists in the Qilian region, suggesting that the back-arc spreading center may have existed for at least 40 Myr and its spreading may have stopped when the Qilian Ocean was closed (subduction ceased as a result).

7.4. Timing for continental collision and mountain building

Several lines of evidence indicate the closure of the Qilian Ocean and subduction cessation at ~445 Ma, the end of Ordovician. This includes (1) the latest arc volcanic rock is 446 ± 3 Ma (Wang et al., 2005), (2) the reliable Ar–Ar plateau ages of phengitic mica from high-grade blueschist belt are 446–454 Ma (Liou et al., 1989; Liu et al., 2006), and (3) Silurian flysh formation that deposited in a shrinked remnant sea was mainly developed in an Ordovician back-arc basin.

Intensive orogenic or mountain building epoch is marked by the Lower Devonian intermontane molasse well developed throughout the North Qilian orogenic belt. This molasse formation laid unconformably over the Silurian flysh and the Cambrain to Ordovician MORB and SSZ ophiolites, arc volcanic complex and HPM rocks. Uplift of mountain chains of the Qilian Orogeny can be interpreted as resulting from continental collision between Alashan block and Qilian–Qaidam block. This collision, however, is little recorded in rocks within the Qilian orogenic belt except for the Devonian molasse. Ar–Ar age of 417 Ma of the low-grade blueschist (Lin et al., 2010) and zircon retrograde ages at 404–424 Ma (Fig. 20) in eclogite samples is consistent with the molasse formation, and would represent the intense period of mountain building (Song et al., 2009a). This period is also consistent with the UHPM and exhumation ages of the North Qaidam continental-type subduction-zone inferred from dating of zircons from garnet-peridotites and coesite-bearing metapelites (~430–400 Ma, Song et al., 2005, 2006).

Just like the Himalaya and Tibet, the HP-UHPM belt, as a result of continental subduction/exhumation, is exposed along the Higher Himalaya (Pakistan, India and Nepal). It is spatially *not* combined in

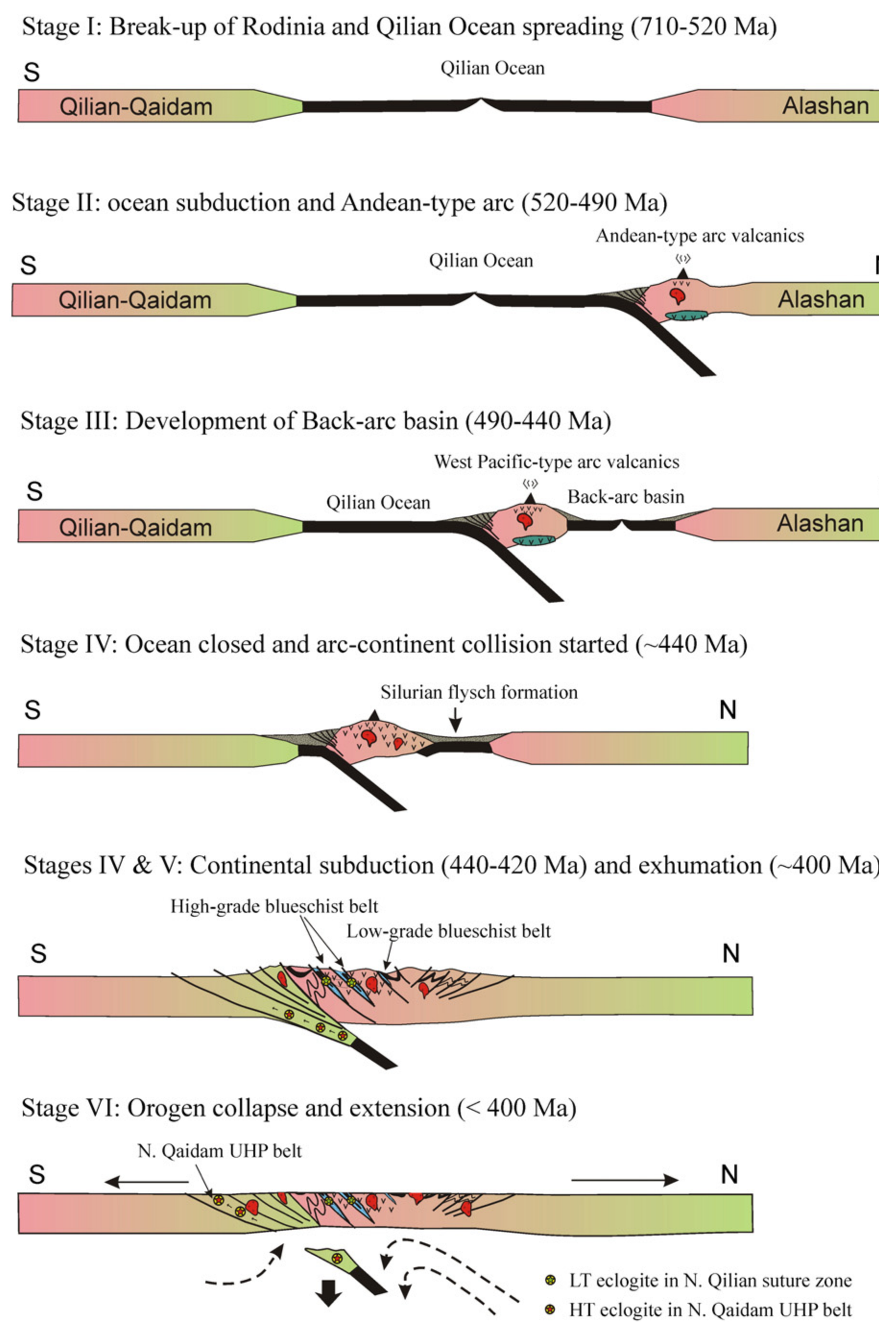

Fig. 22. Tectonic evolution of Qilian Orogen in six stages from Neoproterozoic to Paleozoic time.

the same belt with the oceanic suture zone along the Yaluzangbo River. This phenomenon is most likely attributed to the different exhumation path and mechanism between the subducted oceanic and continent crusts. This architecture can simply explain the tectonic pattern in the Early Paleozoic to be a united convergent zone from oceanic subduction (the Qilian suture zone) to continental subduction/collision (the North Qaidam UHPM belt) as proposed by Song et al. (2006).

7.5. Tectonic evolution of the Qilian Orogen

On the basis of different configurations of arc magmatism, ophiolites, HP-UHP metamorphic rocks, sedimentary basins and detrital zircon geochronology, several tectonic models have been proposed for the North Qilian suture zone and adjacent regions; this includes southward subduction model (e.g., Gehrels et al., 2011; Gehrels and Yin, 2003; Yin et al., 2007; Xiao et al., 2009), northward subduction model (e.g., Xia et al., 1995a, 1995b, 2003; Feng and He, 1996; Yang et al., 2002; Song et al., 2006) and bidirectional subduction model (e.g., Zuo and Liu, 1987; Wu et al., 2010). However, a sensible tectonic model for continental orogenic belts must be based on a comprehensive consideration of all aspects of geological evidence.

On the basis of the foregoing discussions, the inferred tectonic evolution of the Qilian Orogen from ocean opening, initiation of seafloor subduction, development of arc and back-arc system, to continental collision and mountain building is illustrated in Fig. 22 in six major stages.

Stage I (opening of the Qilian Ocean at ~710–520 Ma): As a consequence of break-up of supercontinent Rodinia, the Qilian Ocean opened in the Neoproterozoic (~710 Ma?) as a branch of the worldwide Iapetus Ocean with Atlantic-type passive margins. This ocean kept steady spreading before seafloor subduction began.

Stage II (initiation of subduction and infant arc magmatism at ~520–490): When the oceanic lithosphere was old, cold and sufficiently dense, it began spontaneously to subduct northward beneath the Alashan block at ~520 Ma. As a result, "infant arc" magmatism took place though partial melting of the least depleted mantle wedge, producing MORB-like basaltic rocks. Underplating of arc basaltic magmas caused crustal melting of the Andean-type active continental margin and formed the S-type Chaidano granite intrusion at 516–508 Ma. With increasing the degree of partial melting of the mantle wedge, more refractory melts (boninites) were produced at ~490 Ma.

Stage III (extension of back-arc and SSZ ophiolite formation at ~490–440 Ma): The back-arc region under extension may start to develop back-arc basin at ~490 Ma and produce back-arc ocean crust (the North SSZ-type ophiolite belt) in the period of ~490–440 Ma. Part of the active margin splitted from the continental Alashan block and the Andean-type active margin was thus converted to a Western Pacific-type trench–arc–back-arc system. Simultaneously, LT-HP metamorphic rocks including eclogite and blueschist formed along a cold geothermal gradient of ~6–7 °C/km in the subduction zone (Song et al., 2007; Zhang et al., 2007; Wei and Song 2008; Wei et al., 2009). Cu–Pb–Zn sulfide ore deposits mainly formed in the arc volcanic rocks at this stage.

Stage IV (closure of Qilian Ocean and Silurian flysh formation at ~440–420 Ma): The Qilian Ocean was closed and the back-arc spreading stopped at the end of Ordovician. Continental blocks started to collide and the Qilian–Qaidam block was dragged beneath the Alashan block by the downgoing oceanic lithosphere to depths of ~100–200 km at about 430–420 Ma (Song et al., 2005, 2006). The surface of the suture zone was relatively placid; thick flysch formation deposited in the shrinked remnant back-arc basin in the early Silurian.

Stage V (Uplift of mountain chain and exhumation of subducted crust in the Late Silurian to Early Devonian): subducted continental crust started to exhume along the thrust faults as a result of ocean lithosphere breakoff, and intensive orogenesis occurred in the Late Silurian and Devonian, which led to the mountain-building, HPM rock exhumation and molasse deposition followed as a result in the early Devonian.

Stage VI (Post-orogenic extension and erosion at <400 Ma): In the late Devonian, the Qilian orogenic belt started to collapse; continuous extension causes the mantle upwelling and crust melting to form post-collisional granite intrusions in the southern margin of the Alashan block. In the Carboniferous, orogenic movement totally ceased and marine and marine-continental transition facies sedimentary layers covered all the complexes in the North Qilian orogenic belt. Re-building of the mountains continued as a result of the India-Asia collision in the Cenozoic.

Acknowledgements

This study was supported by the Major State Basic Research Development Projects (2009CB825007), National Natural Science Foundation of China (Grant Nos. 40825007, 40821002, 40773012, 41130314, 91014003) and Basic geological survey program of China Geological Survey (1212011121258, 1212010911070). We thank the two anonymous reviewers and the guest editor Y.F. Zheng for their detailed and constructive comments, which led to a better presentation of the final product.

References

Bexell, G., 1935. On the stratigraphy of the plant-bearing deposit of Late Palaeozoic and Mesozoic age in the Nanshan region (Kansu). Geografiska Annular 17, 62–64.
Bian, Q.T., 1989. The geological structure and metallogenetic model of Baiyin Chang mining area. Seismic Publishing, Beijing. (in Chinese).
Burke, K., Dewey, J.F., Kidd, W.S.F., 1976. Precambrian paleomagnetic results compatible with contemporary operation of the Wilson cycle. Tectonophysics 33, 287–299.
Chai, G., Naldrett, A.J., 1992. The Jinchuan ultramafic intrusion: cumulate of a high-Mg basaltic magma. Journal of Petrology 33, 277–304.
Cao, Y., Song, S.G., 2009. Deformation and metamorphism of HP belt in the North Qilian Mountains and their implications for exhumation. Acta Petrologica Sinica 25, 2235–2246.
Cao, Y., Song, S.G., Niu, Y.L., Jung, H., Jin, Z.M., 2011. Variation of mineral composition, fabric and oxygen fugacity from massive to foliated eclogites during exhumation of subducted ocean crust in the North Qilian suture zone, NW China. Journal of Metamorphic Geology 29, 699–720.
Chen, D.L., Liu, L., Sun, Y., 2009a. Geochemistry and zircon U–Pb dating and its implications of the Yukahe HP/UHP terrane, the North Qaidam, NW China. Journal of Asian Earth Sciences 35, 259–272.
Chen, M.X., 1950. Review on metamorphic sequences in the middle part of Gansu. Geological Review 15, 7–12 (in Chinese).
Chen, N.S., Wang, Q.Y., Chen, Q., Li, X.Y., 2007. Components and metamorphism of the basements of the Qaidam and Oulongbuluke micro-continental blocks, and a tentative interpretation of paleocontinental evolution in NW–Central China. Earth Science Frontiers 14, 43–55 (in Chinese with English abstract).
Chen, N.S., Gong, S.L., Sun, M., Li, X.Y., Xia, X.P., Wang, Q.Y., Wu, F.Y., Xu, P., 2009b. Precambrian evolution of the Quanji Block, northeastern margin of Tibet: insights from zircon U–Pb and Lu–Hf isotope compositions. Journal of Asian Earth Sciences 35, 367–376.
Chen, X., 1957. Features and origin of iron deposits in the Qilian Mountains. Geological Review 17, 218 (in Chinese).
Chen, Y., Zhou, D.J., Wang, E.C., Li, X.Y., 1995. Geochemical characteristics of boninite series rocks found in Dachadaban ophiolite, Sunan County, North Qilian Mountains. Acta Petrologica Sinica 11, 145–153 (in Chinese with English abstract).
Chen, Y.X., Song, S.G., Xia, X.H., in press. Petrogenesis of Aoyougou high-silica adakite in the western sector of the North Qilian Mountain, NW China: evidence for decompression melting of oceanic slab. Science in China.
Chi, Y.S., 1935. Note on two aseptate corals from the upper part of the Nanshan Series in Gansu. Bulletin of the Geological Society of China 14, 47–52.
Coleman, R.G., 1977. Ophiolites. Springer-Verlag, Berlin, Heidelberg, New York. 229p.
Condie, K.C., 1997. Plate Tectonics and Crustal Evolution (Fourth edition). Butterworth-Heinemann, Oxford. 282 pp.
Dick, H.J.B., 1989. Abyssal periodotites, very slow spreading ridges and ocean ridge magmatism. In: Saunders, A.D., Norry, M.J. (Eds.), Magmatism in the Ocean Basins. Geological Society, London, Special Publications, vol. 42, pp. 71–105.
Du Rietz, T., 1940. Igneous rocks of the Nanshan. A study in Caledonian igneous rocks. In: Hedin, S. (Ed.), The Sino-Swidish Expedition, Publication 12, Geology, Part 4 3. Thule, Stockholm, pp. 1–117.
Erickson, S.G., 1993. Sedimentary loading, lithospheric flexure, and subduction initiation at passive margins. Geology 21, 125–128.

Feng, Y.M., He, S.P., 1995a. Research for geology and geochemistry of several ophiolites in the North Qilian Mountains, China. Geological Review 40, 252–264 (in Chinese with English abstract).
Feng, Y.M., He, S.P., 1995b. Basic characteristics of tectonics in the Qilian Mountains and its neighbourings—on genetic environments of Early Paleozoic marine volcanics. Northwest Geoseience 16, 92–103 (in Chinese with English abstract).
Feng, Y.M., Wu, H.Q., 1992. Tectonic evolution of North Qilian Mountains and its neighbourhood since Paleozoic. Northwest Geoscience 13, 61–73 (in Chinese with English abstract).
Feng, Y.M., He, S.P., 1996. Geotectonics and orogeny of the Qilian Mountains (in Chinese). Geological Publish House, Beijing. 135p.
Gehrels, G.E., Yin, A., 2003. Magmatic history of the northeastern Tibetan Plateau. Journal of Geophysical Research 108 (B9), 2423.
Gehrels, G., Kapp, P., DeCelles, P., Pullen, A., Blakey, R., Weislogel, A., Ding, L., Guynn, J., Martin, A., McQuarrie, N., Yin, A., 2011. Detrital zircon geochronology of pre-Tertiary strata in the Tibetan-Himalayan orogen. Tectonics 30, TC5016–TC.
Geng, Y.-S., Wang, X.-S., Shen, Q.-H., Wu, C.-M., 2002. The discovery of Neoproterozoic Jinningian deformed granites in Alax area and its significance. Acta Petorlogica et Mineralogica 21, 412–420 (in Chinese with English abstract).
Geng, Y.-S., Wang, X.S., Shen, Q.H., Wu, C.M., 2006. Redefinition of the Alxa Group-complex (Precambrian metamorphic basement) in the Alxa area, Inner Mongolia. Geology in China 33, 138–145 (in Chinese with English abstract).
Geng, Y.-S., Wang, X.S., Shen, Q.H., Wu, C.M., 2007. Chronology of the Precambrian metamorphic series the Alxa area, Inner Mongolia. Geology in China 34, 251–261 (in Chinese with English abstract).
Guo, J.J., Zhao, F.Q., Li, H.K., 1999. Jinningian collisional granite belt in the eastern sector of the Central Qilian Massif and its implication. Acta Geoscientia Sinica 20, 10–15 (in Chinese with English abstract).
Guo, Z.S., 1948. The time range of Nanshan Series. Geological Review 13, 251–252 (in Chinese).
Gurnis, M., Hall, C., Lavier, L., 2004. Evolving force balance during incipient subduction. Geochemistry, Geophysics, Geosystems 5, 1–31.
He, C.S., 1946. A review on coal geology in Gansu. Geological Review 11, 171–198 (in Chinese).
He, S.P., Wang, H.L., Chen, J.L., Xu, X.Y., Zhang, H.F., Ren, G.M., Yu, J.Y., 2006. A LA-ICP-MS U–Pb chronological study of zircons from meta-acidic volcanics in Baiyin ore-field, Gansu Province: new evidence for metallogenic age of Baiyin type massive sulfide deposits. Mineral Deposits 25, 401–411.
Hou, Q.Y., Zhao, Z.D., Zhang, H.F., et al., 2006. Indian Ocean-MORB-type isotopic signature of Yushigou Ophiolite in north Qilian Mountains and its implications. Science in China Series D-Earth Science 49 (6), 561–572.
Hou, T.F., Sun, C.C., 1935. A geological section northwest of Lanzhou. Bulletin of the Geological Society of China 14, 211–219.
Hu, H.M., 1959. Metallic ore deposits in volcanic series in the east part of the Qilian Mountains. Geological Review 19, 1–12 (in Chinese).
Hu, H.M., Wang, W.G., Sun, X.Q., 1958. Pyritic-copper deposits and exploration in the Qilian Mountains. Geological Review 18, 295–301 (in Chinese).
Hu, N.G., Xu, A.D., Yang, J.X., 2005. Characteristics and tectonic environment of Zhigoumen pluton in Longshoushan area. Journal of Earth Sciences and Environment 27, 5–11 (in Chinese with English abstract).
Hu, N.G., Su, J.P., Zhang, H.F., Feng, B.Z., 2006. Geochemical characteristics petrogenesis of Jinfosi Pluton in Qilian Mountains. Journal of Earth Sciences and Environment 28, 5–12 (in Chinese with English abstract).
Huang, T.K., 1945. On major tectonic forms of China. Geological Memoirs, series A 20, 1–165.
Huang, T.K., 1955. Tectonic pattern and oil-hunting direction on the west margin of Erdos Platform. Acta Geologica Sinica 35, 23–31 (in Chinese).
Institute of Geology of Chinese Academy of Sciences, 1960. Lanzhou Institute of Geology, Beijing College of Geology. Qilian Geology, Vol. I. Science Press, Beijing (in Chinese).
Institute of Geology of Chinese Academy of Sciences, 1963. Lanzhou Institute of Geology, Beijing College of Geology. Qilian Geology., Vol. II. Science press, Beijing (in Chinese).
Jiang, C.F., Wang, Z.Q., Li, J.Y., et al., 2000. Opening Closing Tectonics of Central Orogenic Belt. Geological Publishing House, Beijing, pp. 1–154 (in Chinese).
Lee, J.S., 1939. The Geology of China. Thomas Murby and Co., London. 528 pp.
Lee, J.S., 1954. Vortex structure and the relevant problem on composite of tectonic systems in the northwestern China. Acta Geologica Sinica 34, 340–410 (in Chinese).
Li, C.Y., Liu, Y.W., Zhu, B.C., Feng, Y.M., Wu, H.Q., 1978. Structural evolutions of Qinling and Qilian. In: Scientific Papers on Geology for International Exchange (eds Editorial Office of Chinese Geological Bureau), pp. 174–189. Geological Publishing House, Beijing (in Chinese with English abstract).
Li, J.J., Shen, B.F., Li, H.M., 2004a. Single zircon U–Pb age of granodioritic gneiss in the Bayan Ul area, western Inner Mongolia. Geological Bulletin of China 23 (12), 1243–1245 (in Chinese with English abstract).
Li, S.H., 1946a. A stratigraphical section in Chouniugou, Wuwei, Gansu. Geology Review 11, 207–214 (in Chinese).
Li, S.H., 1946b. Intermediate and basic volcanic rocks in Gansu. Geological Review 11, 217–223 (in Chinese).
Li, S.H., 1948a. Some problems on stratigraphy and orogeny of the Nanshan region. Bulletin of the Geological Society of China 28, 187–200.
Li, S.H., 1948b. An ancient unconformity in the Nanshan region-representing the Caledonian movement. Geological Review 13, 151–152 (in Chinese).
Li, X.H., Su, L., Song, B., Liu, D.Y., 2004b. SHRIMP U–Pb zircon age of the Jinchuan ultramafic intrusion and its geological significance. Chinese Science Bulletin 49, 420–422.
Li, X.H., Su, L., Chung, S.L., Li, Z.X., Liu, Y., Song, B., Liu, D.Y., 2005. Formation of the Jinchuan ultramafic intrusion and the world's third largest Ni–Cu sulfide deposit: associated with the similar to 825 Ma south China mantle plume? Geochemistry, Geophysics, Geosystems 6, Q11004. doi:10.1029/2005GC001006.
Li, X.M., Ma, Z.P., Sun, J.M., Yu, J.Y., 2009a. A LA-ICP-MS chronological study of basic volcanics in Baiyin orefield, Gansu, China. Geological Bulletin of China 28 (7), 901–906 (in Chinese with English abstract).
Li, Y., Fu, G.M., Miao, Q., Li, L., 2009b. The geochemical characteristic for medio-basic volcanic rock from Baiyin area, Gansu Province. Journal of Lanzhou University (Natural Sciences) 45, 55–60 (in Chinese with English abstract).
Li, Z.X., Bogdanova, S.V., Collins, A.S., Davidson, A., De Waele, B., Ernst, R.E., Fitzsimons, I.C.W., Fuck, R.A., Gladkochub, D.P., Jacobs, J., Karlstrom, K.E., Lu, S., Natapov, L.M., Pease, V., Pisarevsky, S.A., Thrane, K., Vernikovsky, V., 2008. Assembly, configuration, and breakup history of Rodinia: a synthesis. Precambrian Research 160, 179–210.
Liang, W.Y., 1949. The cemo-movemnt in the west part of the Qilian Mountains. Geological Review 14, 184–191 (in Chinese).
Lin, Y.H., Zhang, L.F., Ji, J.Q., Song, S.G., 2010. $^{40}Ar/^{39}Ar$ age of Jiugequan lawsonite-blueschists in northern Qilian Mountains and its petrologic significance. Chinese Science Bulletin 55, 2021–2027.
Liou, J.G., Wang, X., Coleman, R.G., 1989. Blueschists in major suture zones of China. Tectonics 8, 609–619.
Liu, L., Wang, C., Chen, D.L., Zhang, A., Liou, J.G., 2009. Petrology and geochronology of HP–UHP rocks from the South Altyn Tagh, northwestern China. Journal of Asian Earth Sciences 35, 232–244.
Liu, Y.J., Neubauer, F., Genser, J., Takasu, A., Ge, X.-H., Handler, R., 2006. 40Ar/39Ar ages of blueschist facies pelitic schists from Qingshuigou in the Northern Qilian Mountains, western China. Island Arc 15, 187–198.
Lu, S.N., 2002. Preliminary Study of Precambrian Geology in the North Tibet-Qinghai Plateau. Geological Publishing House, Beijing. 125 pp. (in Chinese).
Lu, Y.H., 1954. Some problems on stratigraphy of the Cambrian and Ordovician in the northwestern China. Acta Geologica Sinica 34, 311–318 (in chinese).
Mao, J.W., Zhang, Z.H., Jian, P., Wang, Z.L., Yang, J.M., Zhang, Z.C., 2000. U–Pb zircon dating of the Yeniutan Granitic Intrusion in the western part of the North Qilian Mountains. Geological Review 46, 616–620.
Mattinson, C.G., Wooden, J.L., Liou, J.G., Bird, D.K., Wu, C.L., 2006. Age and duration of eclogite-facies metamorphism, North Qaidam HP/UHP terrane, western China. American Journal of Science 306, 683–711.
Mattinson, C.G., Menold, C.A., Zhang, J.X., Bird, D.K., 2007. High- and ultrahigh-pressure metamorphism in the North Qaidam and South Altyn Terranes, western China. International Geology Review 49, 969–995.
Mattinson, C.G., Wooden, J.L., Zhang, J.X., Bird, D.K., 2009. Paragneiss zircon geochronology and trace element geochemistry, North Qaidam HP/UHP terrane, western China. Journal of Asian Earth Sciences 35, 298–309.
McKenzie, D.P., 1977. The initiation of trenches: a finite amplitude instability. In: Talwani, M., Pitman, W.C. (Eds.), Island arcs deep sea trenches and back-arc basins: Maurice Ewing Series, Vol. 1, pp. 57–61.
McKerrow, W.S., Dewey, J.F., Scotese, C.R., 1991. The Ordovician and Silurian development of the Iapetus ocean. In: Basset, M.G., et al. (Ed.), The Murchison Symposium: Palaeontological Association of London, Special Papers in Paleontology, 44, pp. 165–178.
McKerrow, W.S., Niocaill, C.M., Dewey, J.F., 2000. The Caledonian Orogeny redefined. Journal of the Geological Society 157, 1149–1154.
Meert, J.G., 2003. A synopsis of events related to the assembly of eastern Gondwana. Tectonophysics 362, 1–40.
Meng, F.C., Zhang, J.X., Kar, C.-M., Li, J.P., 2010. Constraints on the evolution of the North Qilian ocean basin: MOR-type and SSZ-type ophiolites from Dachadaban. Acta Petrologica et Mineralogica 29, 435–466 (in Chinese with English abstract).
Meschede, M., 1986. A method of discriminating between different types of mid-ocean ridge basalts and continental tholeiites with the Nb–Zr–Y diagram. Chemical Geology 56, 207–218.
Metcalfe, I., 1996. Gondwanaland dispersion, Asian accretion and evolution of Eastern Tethys. Australian Journal of Earth Sciences 43 (6), 605–623.
Mueller, S., Phillips, R.J., 1991. On the initiation of subduction. Journal of Geophysical Research 96 (B1), 651–665. doi:10.1029/90JB02237.
Murphy, J.B., Keppie, J.D., Nance, R.Dd., Dostal, J., 2010. Comparative evolution of the Iapetus and Rheic Oceans: a North American perspective. Gondwana Research 17, 482–499.
NBGMR (Ningxia Bureau of Geology and Mineral Resources, 1990. Regional Geology of Ningxia Province. Geological Memoirs of Ministry of Geology and mineral Resources of People's Republic of China. Geological Publishing House, Beijing. 560 pp. (in Chinese).
Niocaill, C.M., van der Pluijm, B.A., Van der Voo, R., 1997. Ordovician paleogeography and the evolution of the Iapetus ocean. Geology 25, 159–162.
Niu, Y.L., Hékinian, R., 1997a. Basaltic liquids and harzburgitic residues in the Garrett Transform: a case study at fast-spreading ridges. Earth and Planetary Science Letters 146, 243–258.
Niu, Y.L., Hékinian, R., 1997b. Spreading rate dependence of the extent of mantle melting beneath ocean ridges. Nature 385, 326–329.
Niu, Y.L., O'Hara, M.J., Pearce, J.A., 2003. Initiation of subduction zones as a consequence of lateral compositional buoyancy contrast within the lithosphere: a petrological perspective. Journal of Petrology 44, 851–866.
Pearce, J.A., Norry, M.J., 1979. Petrogenetic implications of Ti, Zr, Y and Nb variations in volcanic rocks. Contributions to Mineralogy and Petrology 69, 33–47.
Pearce, J.A., 2003. Supra-subduction zone ophiolites: the search for modern analogues. In: Dilek, Y., Newcomb, S. (Eds.), Ophiolite Concept and the Evolution of Geological Thought: Geological Society of America Special Paper, vol. 373, pp. 269–293.
Peng, L.G., Ren, Y.X., Li, Z.P., 1995. Mineralization models of copper polymetallic ore deposits in the Baiyin mining field. Geological Publishing, Beijing, pp. 23–40 (in Chinese).
Powell, R., Holland, T.J.B., Worley, B., 1998. Calculating phase diagrams involving solid solutions via non-linear equations, with examples using THERMOCALC. Journal of Metamorphic Geology 16, 577–588.

Qian, Q., Wang, Y.M., Li, H.M., Jia, X.Q., Han, S., Zhang, Q., 1998. Geochemical characteristics and genesis of diorites from Laohushan. Gansu Province. Acta Petrologica Sinica 14, 520–528 (in Chinese with English abstract).

Qian, Q., Zhang, Q., Sun, X.M., 2001. Tectonic setting and mantle source characteristics of Jiugequan basalts, North Qilian: constraints from trace elements and Nd-isotopes. Acta Petrologica Sinica 17, 385–394 (in Chinese with English abstract).

QBGMR (Qinghai Bureau of Geology and Mineral Resources, 1991. Regional Geology of Qinghai Province. Geological Memoirs of Ministry of Geology and mineral Resources of People's Republic of China, Series 1, Number 24. Geological Publishing House, Beijing. 662 pp. (in Chinese).

Ravna, E.J.K., Terry, M.P., 2004. Geothermobarometry of UHP and HP eclogites and schists—an evaluation of equilibria among garnet–clinopyroxene–kyanite–phengite–coesite/quartz. Journal of Metamorphic Geology 22, 579–592.

Regenauer-Lieb, K., Yuen, D.A., Branlund, J., 2001. The initiation of subduction: criticality by addition of water? Science 294, 578–580.

Sengör, A.M.C., 1984. The cimmeride orogenic system and the tectonics of Eurasia. Geological Society of America, Special paper 195, 82p.

Shervais, J.W., 1982. Ti–V plots and the petrogenesis of modern and ophiolitic lavas. Earth and Planetary Science Letters 59, 101–118.

Shi, R.D., Yang, J.S., Wu, C.L., 2004. First SHRIMP dating for the formation of the Late Sinian Yushigou Ophiolite North Qilian Mountains. Acta Geologica Sinica 78, 649–657 (in Chinese with English abstract).

Smith, A.D., Yang, H.-Y., 2006. The neodymium isotopic and geochemical composition of serpentinites from ophiolitic assemblages in the Qilian fold belt, northwest China. Journal of Asian Earth Sciences 28, 119–132.

Snyder, D.B., Barber, A.J., 1997. Australia–Banda Arc collision as an analogue for early stages in Iapetus closure. Journal of the Geological Society 154, 589–592.

Sobel, E.R., Arnaud, N., 1999. A possible middle Paleozoic suture in the Altyn Tagh, NW China. Tectonics 18 (1), 64–74.

Song, S.G., Wu, H.Q., 1992. Ductile shearing of subduction complex belt in North Qilian Mountains. China. Northwest Geoscience 13, 47–60 (in Chinese with English abstract).

Song, S.G., 1996. Metamorphic geology of blueschists, eclogites and ophiolites in the North Qilian mountains. 30th IGC Field Trip Guide T392. Geological Publishing House, Beijing. 40 pp.

Song, S.G., 1997. Tectonic evolution of subductive complex belts in the North Qilian Mountains. Advance in Earth Sciences 12, 351–365 (in Chinese with English abstract).

Song, S.G., Su, L., 1998. Plastic rheology of the Yushigou mantle peridotite and implications for dynamics of Paleo-Plate movement in the North Qilian Mountains. Acta Geologica Sinica-English edition 72, 131–141.

Song, S.G., Yang, J.S., Xu, Z.Q., Liou, J.G., Shi, R.D., 2003a. Metamorphic evolution of the coesite-bearing ultrahigh-pressure terrane in the North Qaidam, northern Tibet, NW China. Journal of Metamorphic Geology 21, 631–644.

Song, S.G., Yang, J.S., Liou, J.G., Wu, C.L., Shi, R.D., Xu, Z.Q., 2003b. Petrology, geochemistry and isotopic ages of eclogites in the Dulan UHPM terrane, the North Qaidam, NW China. Lithos 70, 195–211.

Song, S.G., Zhang, L.F., Niu, Y.L., 2004a. Ultra-deep origin of garnet peridotite from the North Qaidam ultrahigh-pressure belt, Northern Tibetan Plateau, NW China. American Mineralogist 89, 1330–1336.

Song, S.G., Zhang, L.F., Niu, Y.L., Song, B., Zhang, G.B., Wang, Q.J., 2004b. Zircon U–Pb SHRIMP ages of eclogites from the North Qilian Mountains, NW China and their tectonic implication. Chinese Science Bulletin 49, 848–852.

Song, S.G., Zhang, L.F., Niu, Y.L., Su, L., Jian, P., Liu, D.Y., 2005. Geochronology of diamond-bearing zircons from garnet-peridotite in the North Qaidam UHPM belt, North Tibetan Plateau: a record of complex histories associated with continental collision. Earth and Planetary Science Letters 234, 99–118.

Song, S.G., Zhang, L.F., Niu, Y.L., Su, L., Song, B., Liu, D.Y., 2006. Evolution from oceanic subduction to continental collision: a case study of the Northern Tibetan Plateau inferred from geochemical and geochronological data. Journal of Petrology 47, 435–455.

Song, S.G., Zhang, L.F., Niu, Y.L., Wei, C.J., Liou, J.G., Shu, G.M., 2007. Eclogite and carpholite-bearing meta-pelite in the North Qilian suture zone, NW China: implications for Paleozoic cold oceanic subduction and water transport into mantle. Journal of Metamorphic Geology 25, 547–563.

Song, S.G., Niu, Y., Zhang, L.F., Wei, C.J., Liou, J.G., Su, L., 2009a. Tectonic evolution of Early Paleozoic HP metamorphic rocks in the North Qilian Mountains, NW China: new perspectives. Journal of Asian Earth Sciences 35, 334–353.

Song, S.G., Su, L., Niu, Y., Lai, Y., Zhang, L.F., 2009b. CH4 inclusions in orogenic harzburgite: evidence for reduced slab fluids and implication for redox melting in mantle wedge. Geochimica et Cosmochimica Acta 73, 1737–1754.

Song, S.G., Zhang, G.B., Su, L., Niu, Y.L., Zhang, L.F., 2009c. Two types of peridotite in North Qaidam UHPM belt and their tectonic implications for oceanic and continental subduction: a review. Journal of Asian Earth Sciences 35, 285–297.

Song, S., Su, L., Li, X.-h., Zhang, G., Niu, Y., Zhang, L., 2010. Tracing the 850-Ma continental flood basalts from a piece of subducted continental crust in the North Qaidam UHPM belt, NW China. Precambrian Research 183, 805–816.

Song, Z.B., Ren, Y.X., Li, Z.P., et al., 2004c. A discussion on intrusion epochs of granodiorites along the Bagexia–Heidaban zone in the western part of the North Oilian Mountains. Acta Geoscientica Sinica 25 (2), 205–208 (in Chinese with English abstract).

Stern, R.J., 2004. Subduction initiation: spontaneous and induced. Earth and Planetary Science Letters 226, 275–292.

Su, L., Song, S.G., Wang, Z.H., 1999. CH4-rich fluid inclusions in the Yushigou mantle peridotite and their implications, North Qilian Mountains China. Chinese Science Bulletin 44, 1992–1995.

Sun, C.C., 1936. On the stratigraphy of upper Huangho and Nanshan region. Bulletin of the Geological Society of China 15, 28–35.

Sun, C.C., 1940. Gold deposits in Gansu and Qinghai. Geological Review 5, 243–248 (in Chinese).

Sun, C.C., 1941. Summary of coalfields in the northwestern China. Geological Review 4, 1–9 (in Chinese).

Sun, S.-S., McDonough, W.F., 1989. Chemical and isotopic systematics of oceanic basalt: implications for mantle composition and processes. In: Saunders, A.D., Norry, M.J. (Eds.), Magmatism in the Ocean Basins: Geological Society of London, Special Publication, vol. 42, pp. 313–345.

Sung, S.H., 1949. On the rocks and metamorphism of Peyinchang volcanic series, Kaolan, Gansu. Bulletin of the Geological Society of China 29, 85–91.

Sung, S.H., 1955. Characteristics of pyritic-copper deposits and ore-formig regularity in the Qilian Mountains. Acta Geologica Sinica 35, 1–22 (in Chinese).

Tang, Z., Yang, J., Xu, S., Tao, X., Li, W., 1992. Sm-Nd dating of the Jinchuan ultramafic rock body, Gansu, China. Chines Science Bulletin 37, 1988–1991.

Torsvik, T.H., Smethurst, M.A., Meert, J.G., Van der Voo, R., McKerrow, W.S., Brasier, M.D., Sturt, B.A., Walderhaug, H.J., 1996. Continental break-up and collision in the Neoproterozoic and Palaeozoic—a tale of Baltica and Laurentia. Earth-Science Reviews 40, 229–258.

Torsvik, T.H., 2003. The Rodinia jigsaw puzzle. Science 300, 1379–1381.

Tseng, C.Y., Yang, H.J., Yang, H.Y., Liu, D.Y., Tsai, C.L., Wu, H.Q., Zuo, G.C., 2007. The Dongcaohe ophiolite from the North Qilian Mountains: a fossil oceanic crust of the Paleo-Qilian ocean. Chinese Science Bulletin 52, 2390–2401.

Tseng, C.-Y., Yang, H.-J., Yang, H.-Y., Liu, D.Y., Wu, C.L., Cheng, C.-K., Chen, C.-H., Ker, C.-M., 2009. Continuity of the North Qilian and North Qinling orogenic belts, Central Orogenic System of China: evidence from newly discovered Paleozoic adakitic rocks. Gondwana Research 16, 285–293.

Tseng, C.-Y., Yang, H.-Y., Wan, Y., Liu, D., Wen, D.-J., Lin, T.-C., Tung, K.-A., 2006. Finding of Neoproterozoic (775 Ma) magmatism recorded in metamorphic complexes from the North Qilian orogen: evidence from SHRIMP zircon U–Pb dating. Chinese Science Bulletin 51 (8), 963–970.

Tung, K.A., Yang, H.Y., Liu, D.Y., 2007a. SHRIMP U–Pb geochronology of detrital zircons from the Longshoushan Group and its tectonic significance. Chinese Science Bulletin 52, 1414–1425.

Tung, K.A., Yang, H.J., Yang, H.Y., Liu, D.Y., Zhang, J.X., Wan, Y.S., Tseng, C.Y., 2007b. SHRIMP U–Pb geochronology of the zircons from the Precambrian basement of the Qilian Block and its geological significances. Chinese Science Bulletin 52, 2687–2701.

Tu, K.Z., 1957a. Ore deposit belt in the Qilian Mountains. Bulletin of the Geological Society of China 37 (11), 1–11.

Tu, K.Z., 1957b. Regional geology in the east part of the Qilian Mountains. Bulletin of the Geological Society of China 37 (11), 12–23.

Van der Pluijm, B.A., Johnson, R.J.E., Van der Voo, R., 1990. Early Paleozoic paleogeography and accretionary history of the Newfoundland Appalachians. Geology 18, 898–901.

Van der Voo, R., 1993. Paleomagnetism of the Atlantic, Tethys and Iapetus Oceans. Cambridge University Press. 424 pp.

Wan, Y.S., Xu, Z.Q., Yang, J.S., 2001. Ages and compositions of the Precambrian high-grade basement of the Qilian terrance and its adjacent areas. Acta Geologica Sinica 75, 375–384.

Wang, C.Y., Zhang, Q., Qian, Q., 2005. Geochemistry of the Early Paleozoic Baiyin volcanic rocks (NW China): implications for the tectonic evolution of the North Qilian Orogenic Belt. Journal of Geology 113, 83–94.

Wang, Q., Liu, X.Y., 1976. The ancient oceanic crust and its tectonic implications, North Qilian Mountains, China. Scienta Geologica Sinica (1), 42–55 (in Chinese with English abstract).

Wang, Q., Liu, X.Y., 1981. On Caledonian polycyclic paired metamorphic belts of Qilian Mountains, northwest China. In: Huang, T.K., Li, C.Y. (Eds.), Contributions to Tectonics of China and Adjacent Regions. Geologial Publishing House, Beijing, pp. 92–101 (in Chinese with English abstract).

Wang, Y., 1937. On a new trilobite from Gansu. Bulletin of the Geological Society of China 16, 357–370.

Wang, Y.S., Chen, J.N., 1987. Metamorphic zones and metamorphism in Qinghai Province and its adjacent areas. Geological Publishing House, Beijing. 137 pp. (in Chinese with English abstract).

Wei, C.J., Yang, Y., Su, X.L., Song, S.G., 2009. Metamorphic evolution of low-T eclogite from the North Qilian orogen, NW China: evidence from petrology and calculated phase equilibria in the system NCKFMASHO. Journal of Metamorphic Geology 27, 55–70.

Wei, C.J., Song, S.G., 2008. Chloritoid–glaucophane schist in the north Qilian orogen, NW China: phase equilibria and P–T path from garnet zonation. Journal of Metamorphic Geology 26 (3), 301–316.

Weng, W.P., Lee, T.S., 1946. Preliminary study of the Quaternary glaciation of Nanshan. Bulletin of the Geological Society of China 26, 163–172.

Wu, C.L., Yang, J.S., Yang, H.Y., Wooden, J.L., Shi, R.D., Chen, S.Y., Zheng, Q.G., 2004. Two types of I-type granite dating and geological significance from North Qilian, NW China. Acta Petrologica Sinica 20 (3), 425–432 (in Chinese with English abstract).

Wu, C.L., Yao, S.Z., Zeng, L.S., et al., 2006. Doubel subduction of the Early Paleozoic North Qilian oceanic plate: evidence from granites in the central segment of North Qilian, NW China. Geology in China 33 (6), 1197–1208 (in Chinese with English abstract).

Wu, C.L., Xu, X.Y., Gao, Q.M., Li, X.M., Lei, M., Gao, Y.H., Frost, R.B., Wooden, J.L., 2010. Early Palaezoie granitoid magmatism and tectonic evolution in North Qilian, NW China. Acta Petrologica Sinica 26, 1027–1044 (in Chinese with English abstract).

Wu, H.Q., 1980. The glaucophane-schist of eastern Qinling and northern Qilian mountains in China. Acta Geologica Sinica 3, 195–207 (in Chinese with English abstract).

Wu, H.Q., 1982. Petrology and mineralogy of high pressure metamorphic zones in northern Qilian Qilian, China. Bulletin of Xi'an Institute of Geology and Mineral Resources 4, 5–21 (in Cinese with English abstract).
Wu, H.Q., 1984. Brief description of the high-pressure low-temperature metamorphic belts in China and discussions on some problems about glaucophane and barroisite. Bulletin of Xi'an Institute of Geology and Mineral Resources 7, 63–81 (in Chinese with English abstract).
Wu, H.Q., 1987. Mineralogical and polytypic characteristics of phengite and inspiration for K–Ar ages in Northern Qilian Mountains, China. Bulletin of Xi'an Institute of Geology and Mineral Resoures 15, 22–46 (in Chinese with English abstract).
Wu, H.Q., Feng, Y.M., Huo, Y.G., Zuo, G.Ch., 1990. Discovery of lawsonite glaucophane schist and the signification in Sunan, Gansu, China. Giological Review 36, 277–280 (in Chinese with English Abstract).
Wu, H.Q., Feng, Y.M., Song, S.G., 1993. Metamorphism and deformation of blueschist belts and their tectonic implications, North Qilian Mountains, China. Journal of Metamorphic Geology 11, 523–536.
Wu, H.Q., Song, S.G., 1992. Two types of blueschist and their structural features in North Qilian Mountains. In: Li, Q.B., Dai, J.X., Liu, R.Q., Li, J.L. (Eds.), Symposium of the Researches on Modern Geology, I. Publishing House of Nanjing University, pp. 74–80 (in Chinese with English abstract).
Xia, L.Q., Xia, Z.C., Ren, Y.X., Peng, L.G., Zhang, C., Yang, J.H., Wang, X.A., Li, Zh.P., 1991a. Determination on magmatic properties of the Ordovician island arc volcanic series in Shihuigou, North Qilian Mountains. Acta Petrologica et Mineralogica (1), 1–10 (in Chinese with English abstract).
Xia, L.Q., Xia, Z.C.H., Ren, Y.X., Peng, L.G., Zhang, Ch., Yang, J.H., Wang, X.A., Li, Zh.P., Han, S., Huang, Zh.X., 1991b. Marine Volcanic Rocks from Qilian and Qinling Mountains. China University of Geosciences Press, Wuhan. (in Chinese with English abstract).
Xia, L.Q., Xia, Z.Ch., Xu, X.Y., 1995a. Dynamics of tectono-volcano-magmatic evolution from North Qilian Mountains, China. Northwest Geoscience 16, 1–27 (in Chinese with English abstract).
Xia, L.Q., Xia, Z.C., Xu, X.Y., 1995b. The relationship between marine volcanism and ore-forming process from the end of late Proterozoic era to Cambrian perioe in Northern Qilian Mts. Northwest Geoscience 16, 29–37 (in Chinese with English abstract).
Xia, L.Q., Xia, Z.C., Xu, X.Y., 1996. Petrogenesis of Marine Volcanic Rocks in the North Qilian Mountains. Geological Publish House, Beijing. 153 pp. (in Chinese).
Xia, L.Q., Xia, Z.C., Xu, X.Y., 1998. Early Paleozoic mid-ocean ridge—ocean island and back-arc basin volcanism in the north Qilian mountains. Acta Geologica Sinica 72 (4), 301–312 (in Chinese with English abstract).
Xia, L.Q., Xia, Z.C., Xu, X.Y., 2003. Magmageneisis in the Ordovician in back basins of the northern Qilian Mountains, China. Geological Society of America Bulletin 115, 1510–1522.
Xia, X.H., Song, S.G., 2010. Forming age and tectono-petrogenises of the Jiugequan ophiolite in the North Qilian Mountain, NW China. Chinese Science Bulletin 55, 1899–1907.
Xia, X.H., Song, S.G., Niu, Y.L., in press. Tholeiite-Boninite terrane in the North Qilian suture zone: implications for subduction initiation and back-arc basin development. Chemical Geology doi:10.1016/j.chemgeo.2011.12.001.
Xiang, Z.Q., Lu, S.N., Li, H.K., Li, H.M., Song, B., Zheng, J.K., 2007. SHRIMP U–Pb zir con age of gabbro in Aoyougou in the western segment of the North Qilian Mountains, China and its geological implications. Geological Bulletin of China 26, 1686–1691.
Xiao, W.J., Windley, B.F., Yong, Y., Yan, Z., Yuan, C., Liu, C.Z., Li, J.L., 2009. Early Paleozoic to Devonian multiple-accretionary model for the Qilian Shan, NW China. Journal of Asian Earth Sciences 35, 323–333.
Xiao, X.C., Chen, G.M., Zhu, Z.Z., 1974. Some knowledge about the paleo-plate tectonics of the Qilian Mountains. Geological Seience and Technology 3, 73–78 (in Chinese with English abstract).
Xiao, X.C., Chen, G.M., Zhu, Z.Z., 1978. A preliminary study on the tectonics ancient ophiolites in the Qilian Mountain, northwest China. Acta Geologica Sinica 4, 279–295 (in Chinese with English abstract).
Xiu, Q.Y., Yu, H.F., Li, Q., Zuo, G.C., Li, J.W., Cao, C.J., 2004. Discussion on the petrogenic time of Longshoushan Group, Gansu Province. Acta Geologica Sinica 78, 366–373 (in Chinese with English abstract).
Xu, W.C., Zhang, H.F., Liu, X.M., 2007. U–Pb zircon dating constraints on formation time of Qilian high-grade metamorphic rock and its tectonic implications. Chinese Science Bulletin 52, 531–538.
Xu, Z.Q., Xu, H.F., Zhang, J.X., Li, H.B., Zhu, Z.Z., Qu, J.C., Chen, D.C., Chen, J.L., Yang, K.C., 1994. The Zhoulangnashan Caledonian subductive complex in the Northern Qilian Mountains and its dynamics. Acta Geologica Sinica 68, 1–15 (in Chinese with English abstract).
Yan, J.N., 1955. Introduction for geology in the Qilian Mountains. Geological Knowledge 6, 10–17 (in Chinese).
Yan, Z., Xiao, W.J., Windley, B.F., Wang, Z.Q., Li, J.L., 2010. Silurian clastic sediments in the North Qilian Shan, NW China: chemical and isotopic constraints on their fore-arc provenance with implications for the Paleozoic evolution of the Tibetan Plateau. Sedimentary Geology 231, 98–114.
Yang, J.S., Xu, Z.Q., Zhang, J.X., Chu, J.Y., Zhang, R.Y., Liou, J.G., 2001. Tectonic significance of Caledonian high-pressure rocks in the Qilian–Qaidam–Altun Mountains, NW China. In: Hendrix, Marc S., Davis, Greg A. (Eds.), Paleozoic and Mesozoic tectonic evolution of central Asia: from continental assembly to intracontinental deformation: Geololgical Society of America, Memoir, 194, pp. 151–170.
Yang, J.S., Xu, Z.Q., Zhang, J.X., Song, S.G., Wu, C.L., Shi, R.D., Li, H.B., Brunel, M., 2002. Early Palaeozoic North Qaidam UHP metamorphic belt on the north-eastern Tibetan plateau and a paired subduction model. Terra Nova 14, 397–404.
Yin, A., Manning, C.E., Lovera, O., Menold, C.A., Chen, X., Gehrels, G.E., 2007. Early Paleozoic tectonic and thermomechanical evolution of ultrahigh-pressure (UHP) metamorphic rocks in the Northern Tibetan Plateau, Northwest China. International Geology Review 49, 681–716.
Yin, A., Dang, Y.-Q., Zhang, M., Chen, X.-H., McRivette, M.W., 2008. Cenozoic tectonic evolution of the Qaidam basin and its surrounding regions (part 3): structural geology, sedimentation, and regional tectonic reconstruction. Geological Society of America Bulletin 120, 847–876.
Young, C.C., 1935. On a dorsal fin-spine of Hyodus from Northwestern Gansu. Bulletin of the Geological Society of China 14, 1–10.
Yu, X.N., Song, S.G., Wei, C.J., Zhang, L.F., 2009. Mg-carpholite metapelite and its implications for ancient oceanic subduction in the North Qilian suture zone, NW China. Acta Scientiarum Naturalium Universitatis Pekinensis 45, 472–480.
Yu, S., Zhang, J., Del Real, P.G., 2012. Geochemistry and zircon U–Pb ages of adakitic rocks from the Dulan area of North Qaidam UHP terrane, north Tibet: constraints on the timing and nature of regional tectonothermal events associated with collisional orogeny. Gondwana Research 21, 167–179.
Yuan, P.L., 1925. Carboniferous stratigraphy of northwestern Gansu. Bulletin of the Geological Society of China 4, 6.
Yue, Y.J., Liou, J.G., 1999. Two-stage evolution model for the Altyn Tagh fault. Geology 27, 227–230.
Zhang, D.Q., Sun, G.Y., Xu, H.L., 1995. Petrology and isotope chronology of the Jinfosi pluton, Qilian Mts., Gansu. Acta Geoscientia Sinica 37 (4), 375–385.
Zhang, G.B., Song, S.G., Zhang, L.F., Niu, Y., 2008. The subducted oceanic crust within continental-type UHP metamorphic belt in the North Qaidam, NW China: evidence from petrology, geochemistry and geochronology. Lithos 104, 99–108.
Zhang, J.X., Xu, Z.Q., 1995. Caledonian subduction-accretionary complex/volcanic arc zone and its deformation features in the middle sector of North Qilian Mountains. Acta Geoscientia Sinica (2), 153–163 (in Chinese with English abstract).
Zhang, J.X., Xu, Z.Q., Chen, W., Xu, H.F., 1997a. A tentative discussion on the ages of the subduction-accretionary complex/volcanic arcs in the middle sector of North Qilian Mountain. Acta Petrologica et Mineralogica 16, 112–119 (in Chinese with English abstract).
Zhang, J.X., Zhang, Z.M., Xu, Z.Q., Yang, J.S., Cui, J.W., 2001a. Petrology and geochronology of eclogites from the western segment of the Altyn Tagh, Northwestern China. Lithos 56, 187–206.
Zhang, J.X., Meng, F.C., Wan, Y.S., Yang, J.S., Tung, K.A., 2003a. Early Paleozoic tectonothermal event of the Jingshuikou Group on the South margin of Qaidam: zircon U–Pb SHRIMP age evidence. Geological Bulletin of China 22, 397–404 (in Chinese with English abstract).
Zhang, J.X., Meng, F.C., 2006. Lawsonite-bearing eclogites in the north Qilian and north Altyn Tagh: evidence for cold subduction of oceanic crust. Chinese Science Bulletin 51, 1238–1244.
Zhang, J.X., Yang, J.S., Meng, F.C., Wan, Y.S., Li, H.M., Wu, C.L., 2006. U–Pb isotopic studies of eclogites and their host gneisses in the Xitieshan area of the North Qaidam mountains, western China: new evidence for an early Paleozoic HP–UHP metamorphic belt. Journal of Asian Earth Sciences 28, 143–150.
Zhang, J.X., Meng, F.C., Wan, Y.S., 2007. A cold Early Palaeozoic subduction zone in the North Qilian Mountains, NW China: petrological and U–Pb geochronological constraints. Journal of Metamorphic Geology 25, 285–304.
Zhang, L.F., Wang, Q.J., Song, S.G., 2009. Lawsonite blueschist in Northern Qilian, NW China: PT pseudosections and petrologic implications. Journal of Asian Earth Sciences 35, 345–366.
Zhang, Q., Sun, X., Zhou, D., Qian, Q., Chen, Y., Wang, Y., Jia, X., Han, S., 1997b. The characteristics of North Qilian ophiolites, forming settings and their tectonic significance. Advance in Earth Sciences 12, 366–393 (in Chinese with English abstract).
Zhang, Q., Chen, Y., Zhou, D.J., 1998. Geochemical characteristics and genesis of Dachadaban ophiolite in North Qilian area. Science in China Series D-Earth Science 41 (3), 277–281.
Zhang, Q., Zhou, G.Q., 2001. Ophiolites of China (in Chinese with English abstract). Science Press, Beijing. 182 pp.
Zhang, Q., Zhou, C., Wang, Y., 2003b. The distribution of time and space of Chinese ophiolites and their tectonic settings. Acta Petrologica Sinica 19, 1–8 (in Chinese with English abstract).
Zhang, Z.C., Zhou, M.F., Robinson, P.T., Mao, J.W., Yang, J.M., Zuo, G.C., 2001b. SHRIMP dating of the Aoyougou ophiolite in the west sector of the north Qilian Mountains and its geological significance. Acta Petrologica Sinica 17, 222–226 (in Chinese with English abstract).
Zhang, Z.M., 1989. High pressure-low temperature metamorphism in North Qilian China. In: Cui, G.Z., Shi, B.H. (Eds.), The Exploration for Geological Science of China. Publishing House of Beijing University, pp. 273–295 (in Chinese with English abstract).
Zhang, Z.M., Liou, J.G., 1987. The high P–T metamorphic rocks of China. In: Leitch, E.C., Scheibner, E. (Eds.), Terrane Accretion and Orogenic Belts. Geodynamics Series, Vol.19. American Geophysical Union, Washington, pp. 235–247.
Zhao, G.C., 2009. Metamorphic evolution of major tectonic units in the basement of the North China Craton: key issues and discussion. Acta Petrologica Sinica 25, 1772–1792.
Zuo, G.C., 1986. The early Paleozoic collisional suturing in North Qilian Range, China. Contributions to the project of plate tectonics in northern China, No.1. Geological Publishing House, Beijing, pp. 27–36 (in Chinese with English abstract).
Zuo, G.C., Liu, J.C., 1987. The evolution of tectonics of Early Paleozoic in North Qilian Range. China. Scienta Geologica Sinica 63, 14–24 (in Chinese with English abstract).